Alma Mater Studiorum – Università di Bologna

DOTTORATO DI RICERCA IN

BIOCHIMICA

Ciclo **XXIV**

Settore Concorsuale di afferenza: 05/E1- Biochimica Generale e Biochimica Clinica

Settore Scientifico disciplinare: BIO/10

Effect of hypoxia and hyperglycemia on cell bioenergetics

Presentata da:

Dott.ssa Marianna Del Sole

Coordinatore Dottorato   **Relatore**

Chiar.mo Prof. **Giorgio Lenaz**   *Chiar.mo Prof.* **Giancarlo Solaini**

Esame finale anno 2012

Index

Introduction

Results and Discussion

70 Modulation of ATPase Inhibitory Factor 1 (IF$_1$) expression

Materials and methods

References

Introduction

1 Mitochondria

Structure

Mitochondria are rod-shaped organelles and can be considered the power generators of the cell, converting oxygen and nutrients into adenosine triphosphate (**ATP**). ATP is the chemical energy "currency" of the cell that powers the cell's metabolic activities. Mitochondria, which are found in nearly all eukaryotes, including plants, animals, fungi, and protists, are large enough to be observed with a light microscope and were first discovered in the 1800s. The name of the organelles was coined to reflect the way they looked to the first scientists to observe them, stemming from the Greek words for "thread" and "granule." Mitochondria are usually represented like single entities in the images obtained by electron microscopy (figure 1) but in living cells they appear more like a continuous tubular network, when they are detected by fluorescence microscopy (figure 2).
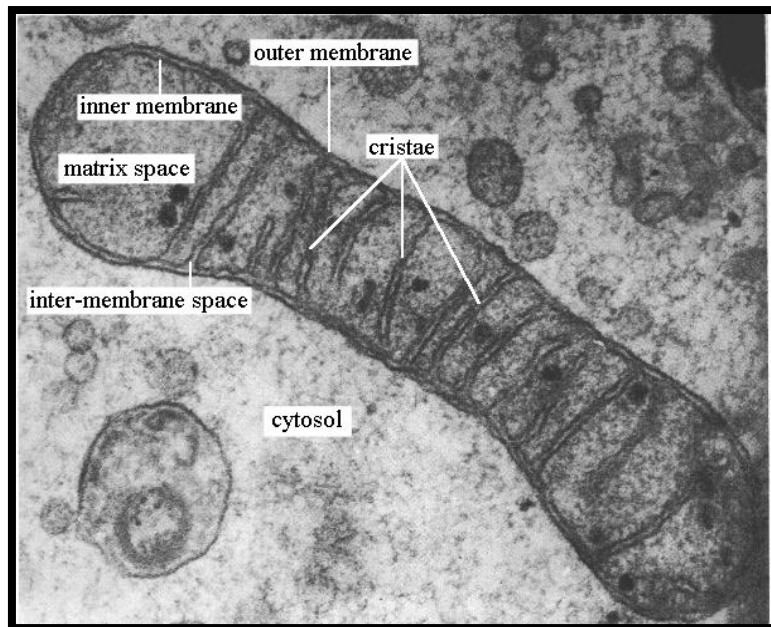
figure 1 Mitochondrion: electron microscopy of a sectional view
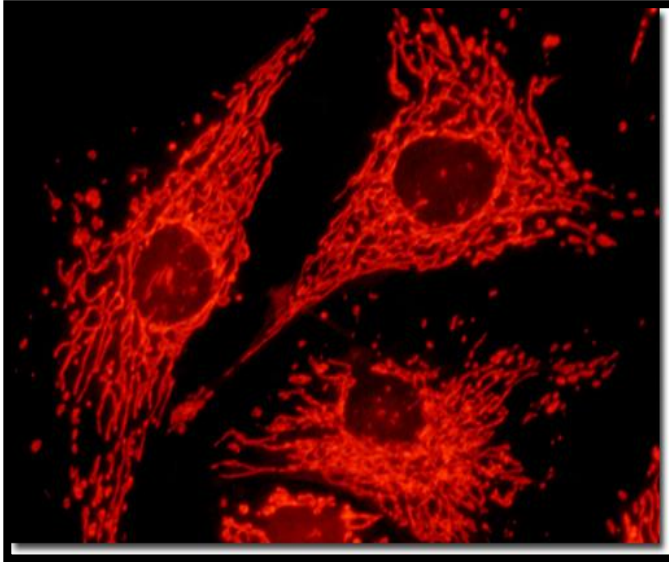
figure 2. Fluorescence emission intensity from a culture of bovine pulmonary artery endothelial cells stained with MitoTracker Red, which targets the intracellular mitochondrial network.

Mitochondria include two phospholipid bilayers with embedded proteins that define four compartments, where different metabolic processes take place: the mitochondrial outer membrane (MOM), the intermembrane space, the mitochondrial inner membrane (MIM) and the matrix (the space enclosed by the inner membrane) (figure 3). It has been estimated that some 1500 different proteins are found in the various mitochondrial compartments where they have specific functions [1].
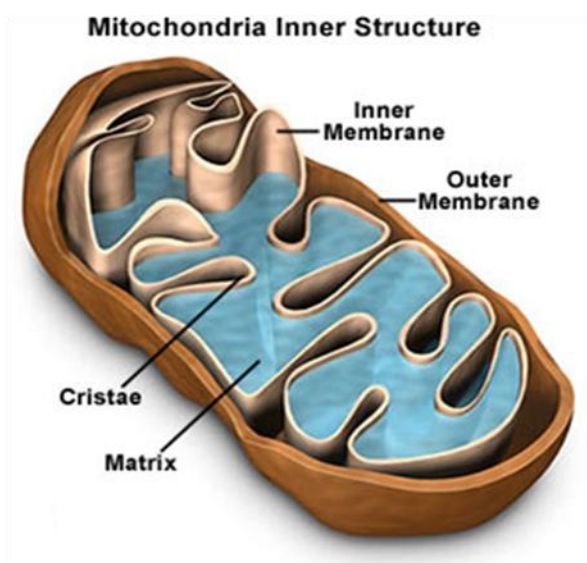
figure 3. Mitochondrion: schematic rapresentation

Proteins localized in the MOM are integral membrane proteins with one or more membrane-spanning regions or membrane-associated peripheral proteins. These membrane proteins are involved in solute exchange between the cytosol and intermembrane space, protein import into mitochondria, docking sites for cytosolic proteins, and uptake of activated fatty acids into the mitochondria]. MOM proteins account for approximately 4% of the total mitochondrial protein [1].

The intermembrane space is delimited by the outer and inner membrane and has a protein composition different from the cytosol and matrix, in part due to the specific amino acid sequences needed to cross the outer as well as the inner membrane. The protein content of this space is much lower than that of the matrix (about 6% of the total mitochondrial protein). The main protein is cytochrome c, which is involved in respiration in normal cells and in apoptosis. Other potential apoptotic inducers are present, as well as enzymes such as adenylate kinase and creatine kinase.

Approximately 21% of the total mitochondrial protein is localized in the MIM. In contrast to the MOM, it has a high protein:phospholipid ratio (more than 3:1 by weight) and is rich in cardiolipin. The MIM is highly impermeable to all anidrous molecules, therefore solutes require specific transporters to enter or exit the matrix [2].

It also contains the translocase of the inner membrane (TIM) complex, which catalyzes the import of proteins into the matrix with the translocase of the outer membrane (TOM) complex.

The inner mitochondrial membrane is compartmentalized into numerous cristae, which expand the surface area of the inner mitochondrial membrane, enhancing its ability to produce ATP. The cristae are invaginations of the inner membrane, which can affect overall chemiosmotic function. The cristae contain the electron transport chain (ETC) complexes (complexes I–IV) and ATP synthetase (complex V). Mitochondria of cells that have greater demand for ATP, such as muscle cells, contain more cristae than liver mitochondria [3].

The matrix is the space enclosed by the inner membrane containing about two-thirds of the total protein in a mitochondrion, it contains a highly concentrated mixture of hundreds of enzymes, in addition to the special mitochondrial ribosomes, tRNA, and several copies of the mtDNA. Most of the enzymes in the matrix are involved in the oxidation of pyruvate and fatty acids and the Krebs cycle [4].

Mitochondrial genome

The mitochondria are ancient bacterial symbionts with their own mitochondrial DNA (mtDNA), RNA, and protein synthesizing systems. Each human cell contains hundreds of mitochondria and thousands of mtDNAs. The mtDNA is maternally inherited and shows striking regional genetic variation. This regional variation was a major factor in permitting humans to adapt to the different global environments they encountered and mastered [5].

mtDNA retains only the genes for the 12S and 16S rRNAs and the 22 tRNAs required for mitochondrial protein synthesis plus 13 polypeptides of the mitochondrial energy generating process, oxidative phosphorylation (OXPHOS). The remaining ~1500 genes of the mtDNA are now scattered throughout the chromosomal DNA. These nDNA-encoded mitochondrial proteins are translated on cytosolic ribosomes and selectively imported into the mitochondrion through various mitochondrial protein import systems [5].

mtDNA is a double-stranded circular DNA molecule of approximately 16.5 kb in all mammals in which it has been sequenced (figure 4). The two strands are referred to as heavy (H) and light (L), reflecting their behavior in density gradients.

figure 4. Human Mitochondrial DNA

The genome is exceedingly compact; there are no introns, and there is only one noncoding (control) region of approximately 1 kb that contains the replication origin for leading strand synthesis (OH), and the promoters for transcription of the H- and L-strands. The mtDNA copy number in somatic cells is generally is about a hundred copies per cell, packaged in a DNA-protein structure called the nucleoid at approximately 2–10 copies per nucleoid [6].

Investigation of the protein constituents of the yeast mitochondrial nucleoid by mass spectrometry has revealed a large number of proteins, some of which have dual functions in nucleoid maintenance and tricarboxylic acid cycle activity [7].

The mitochondrial nucleoid in higher eukaryotes is reported to contain TFAM, a mitochondrial transcription factor, single-stranded binding protein, Twinkle (a helicase), and at least four additional inner membrane proteins. TFAM is a basic protein of the HMG box family that is thought to package mtDNA. Decreasing TFAM levels results in loss of mtDNA [6].

Mitochondrial Oxidative Phosphorylation

In most human tissues, mitochondria provide the energy necessary for cell growth, and biological activities. It has been estimated that 90% of

mammalian oxygen consumption is mitochondrial, which primarily serves to synthesize ATP, although in variable levels according to the tissue considered and the organism's activity status.

Mitochondria intervene in the ultimate phase of cellular catabolism, following the enzymatic reactions of intermediate metabolism that degrade carbohydrates, fats, and proteins into smaller molecules such as pyruvate, fatty acids, and amino acids.

Mitochondria further transform these energetic elements into NADH and/or FADH2, through β-oxidation and the Krebs cycle. Those reduced equivalents are then degraded by the mitochondrial respiratory chain in a global energy converting process called oxidative phosphorylation (OXPHOS), where the electrons liberated by the oxidation of NADH and FADH2 are passed along a series of carriers regrouped under the name of "respiratory chain" or "electron transport chain" (ETC) , and ultimately transferred to molecular oxygen. ETC is located in the mitochondrial inner membrane, with an enrichment in the cristae. ETC consists of four enzyme complexes (complexes I to IV), and two mobile electron carriers (coenzyme Q and cytochrome c). These complexes are composed of numerous subunits encoded by both nuclear genes and mitochondrial DNA at the exception of complex II (nuclear only) [2].

ETC complexes transfer electrons deriving from NADH and FADH2 to molecular oxygen producing water (figure 5). The oxygen reduction occurs through a multi-steps process: **Complex I** *(NADH:Ubiquinone oxidoreductase)* or Complex II *(Succinate:Ubiquinone oxidoreductase)* transfer two electrons deriving from NADH or FADH2 to CoQ giving ubisemiquinone (CoQ•) and then ubiquinol (CoQH2).

Complex II is the only enzyme of respiratory chain that does not show proton-pumping activity but it represents an alternative entry point for electrons and a checkpoint for the coordination between Krebs cycle and oxidative phosphorylation [8]**.**

Complex II is composed of four subunits all encoded by nuclear genes: the two largest subunits lie in the matrix space and contain a covalently bound flavine adenine dinucleotide together with three Fe-S clusters. The other two subunits, less conserved, are localized in the membrane and contain a type *b* heme and two ubiquinone/ubiquinol binding domains localized on opposite sites of the inner membrane. The large distance between the two quinones would suggest that only the quinone bound near the cytplasmic side of inner membrane is part of the electron transfer chain. The catalytic mechanism consists in the reduction of FAD by the succinate molecule followed by electron transfer to CoQ through the Fe-S clusters chain. The role of heme *b* is not yet clearly understood. Besides its potential structural role, this prosthetic group could take part to redox reactions only during reverse electron transfer, being capable to participate in fumarate reduction but not in succinate oxidation [9-10]**.**

Ubiquinol is oxidized by **Complex III** *(Ubiquinol:Cytochrome c oxidoreductase)* which reduces cytochrome *c*. Complex III exists as symmetric dimer where each monomer consists of eleven subunits.
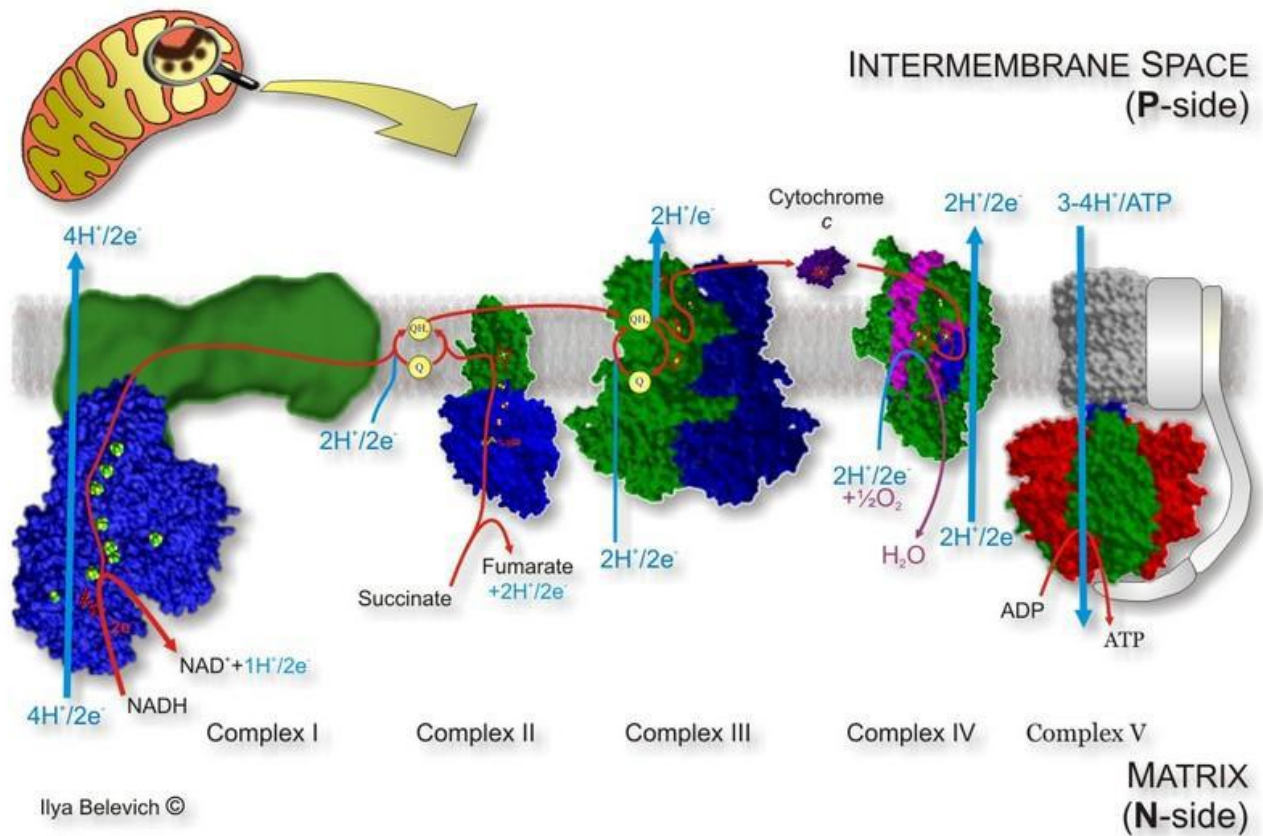
figure 5. Schematic representation of OXPHOS system (from *Helsinki Bioenergetics Group, Institute of Biotechnology, Finland*).

The catalytic core is formed by three subunits containing all the redox centers of the enzyme: cytochrome *b*, cytochrome *c*1 and an iron-sulfur protein known as Rieske protein. Cytochrome *b* contains two heme groups – *b*565 and *b*560 – and two ubiquinone/ubiquinol binding sites called P center and N center; cytochrome *c*1 is the cytochrome *c* electron donor. The redox proteins along with other three subunits [11] **(OMIM- Online Mendelian Inheritance in Man)** span the inner membrane while the remaining subunits are exposed to the matrix or to the intermembrane space. The catalytic mechanism is characterized by oxidation of ubiquinol and reduction of ubiquinone during the Q-Cycle. This process allows the translocation of four protons across the membrane and it occurs through one-electron steps oxidation of ubiquinol. Briefly, one electron deriving from the ubiquinol on the P 10 center sequentially flows from the high-potential Fe2-S2 cluster to cytochrome *c*1 and cytochrome *c*. The ubiquinol oxidation is completed through a different pathway: the second electron reduces heme *b*560, heme *b*565 and finally a molecule of ubiquinone bound at the N center to its ubisemiquinone form.

The cycle ends with the binding of a second CoQH2 at the P center: in this case, the first electron is used to reduce a second cytochrome *c* molecule while the other flows through heme *b*565 and *b*560 to reduce the ubisemiquinone at the N center determining the uptake of two protons from the matrix. The complete reaction can be so represented:

$$QH_2 + 2 \text{ cyt } c_{ox} + 2H^+_{matrix} \rightarrow Q + 2 \text{ cyt } c_{red} + 4H^+_{intermembrane \text{ } space}$$
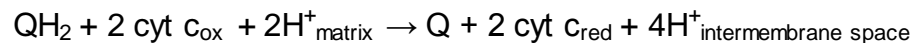
From cytochrome *c* electrons flow to **Complex IV** *(Cytochrome c oxidase)* that finally reduces molecular oxygen to water. Complex IV is composed of thirteen subunits; three of them - I, II and III - are encoded by mitochondrial genes and represent the catalytic core of the enzyme. In subunit I are localized a copper atom - CuB - and two heme groups, called *a* and *a*3. Subunit II contains CuA, a binuclear copper center. The catalytic action occurs through Cytochrome *c* oxidation by CuA. Heme *a* represents the bridge between CuA and the heme-copper center formed by CuB and heme *a*3 where molecular oxygen is bound and reduced to water [12]**.**

Nevertheless subunit III is well conserved during evolution, its function still remains uncertain: the absence of redox centers excludes its participation to electron transfer. Moreover, studies in *P. denitrificans* have showed that a cytochrome oxidase lacking of subunit III conserves the capacity of translocate protons suggesting that this subunit is not determinant for proton pumping.

The oxygen reduction by Complex IV occurs through a multi-steps mechanism in which different iron-oxygen intermediates are formed thanks to the cooperation between heme *a*3 and CuB. The electron transfer is coupled with the uptake of an equal number of protons from the matrix so that for each complete cycle four protons are vectorially translocated into the intermembrane space. The complex is provided with three potential channels by which proton transport can be accomplished. The so-called K channel allows the access of the four protons to the binuclear site for water formation, whereas D and H channels span the entire membrane layer. These channels

are characterized by amino acids with protonable side chain, capable to form hydrogen bonds with nearby amino acids and to create a bridge between the matrix and the intermembrane space. However, site-directed mutagenesis studies, performed with the bacterial enzyme, suggest that the H channel is not involved in proton translocation. The nuclear-encoded subunits exposed ether to the matrix or to the intermembrane space, are not directly involved in the catalytic mechanism and are supposed to have a regulatory function [13].

The energy released by the exergonic electron transfer to the oxygen is then converted in what P. Mitchell, who first proposed the chemiosmotic theory, called **protonmotive force**. Contextually to the redox reactions Complex I, III and IV pump protons from the matrix into the intermembrane space so that through the inner membrane is established an electrochemical gradient (ΔP) consisting of two components: ΔΨ (electric) and ΔpH (chemical).

Complex V *(ATP synthase)* converts the energy stored in ΔP in high-energy phosphate bonds readily available for cell demand. Complex V F0 sector, embedded in the inner membrane, contains a channel that allows to protons to flow back to the matrix thanks to the electrochemical gradient. The energy released by ΔP dissipation is linked to ATP synthesis by the Complex V soluble portion, F1, through a tree steps mechanism in which ADP and Pi are bound and condensed to form ATP that is finally released into the matrix. The mammalian F0 component contains nine subunits (a, b, c, d, e, f, g, A6L, F6), while the F1 hydrophilic component has a α3, β3, γ, δ, ε composition where β subunits represent the active sites for the ATP synthesis. In the inner membrane 8-12 c subunits are arranged in a ring connected by a stalk to the catalytic component in the hydrophilic portion. The γ, δ and ε subunits compose the central part of the stalk moiety, while the peripheral stalk, lying to one side of the complex is composed of b, d, F6 and OSCP (oligomycin sensitivity conferring protein) subunits [13].

Complex V works as a rotary motor in which the protons flow through the F0 portion modulates the properties of the β subunits. The catalytic subunits exist in three different conformations associated with different affinity for ADP-Pi and ATP, according to the binding-change mechanism proposed by Boyer [14].

The energy deriving from proton gradient dissipation is actually needed to eliminate the strong interaction between the newly synthesized ATP and the catalytic site. The transition between the three different β conformations is driven by the rotation of γ subunit. The b subunit along with other stalk components works as a tether between the F0 and the α3-β3 module inducing the distortion of the β subunits in response to the rotor (c-ring, γ, δ, ε) motion. The proton channel is supposed to be localized in the interface between a and c subunits and the translocation is likely achieved by amino acids provided with carboxylate groups whose electrostatic interactions drive the rotor [13].

IF1, the endogenous mitochondrial ATP hydrolase inhibitor

In normally respiring mitochondria, the removal of ATP by the adenine nucleotide translocase (ANT) ensures that the intra-mitochondrial phosphorylation potential is held relatively low while $\Delta\psi_m$ is high, favouring ADP phosphorylation (i.e. ATP synthesis). When mitochondrial homeostasis is compromised, the situation can reverse. A decrease in $\Delta\psi_m$ accompanied by an increase in the phosphorylation potential, as glycolysis is upregulated together with reversal of the ANT, which imports glycolytic ATP, will favour ATP hydrolysis **(Fig 6a(i))**.

Therefore, during mitochondrial dysfunction caused by mutations in mtDNA genes, the F1Fo-ATPase can run 'backwards', acting as an ATP-consuming proton pump **(Fig 6a(ii))**.
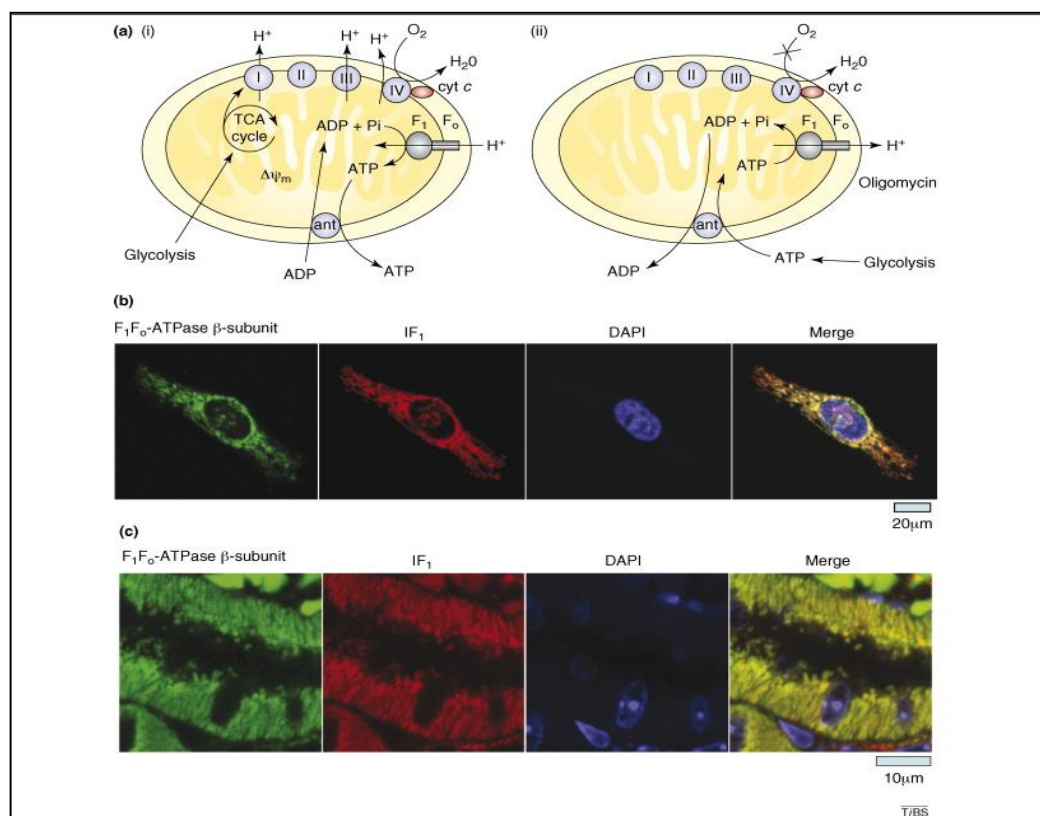
Figura 5. Role of F1Fo-ATP synthase in mitochondrial bio-energetics. F1Fo-ATP synthase activity and co-localisation with IF1 are depicted. (a) Cartoons illustrating the operations of the F1Fo-ATP synthase in (i) respiring mitochondria and (ii) mitochondria acting as ATP consumers. Panels (b) and (c) illustrate the mitochondrial co-localisation of IF1 (red) with the b-subunit of the F1Fo-ATP synthase (green) using immunofluorescence of the HeLa cell line

14

(b) and intact rat kidney (c). DAPI staining of the nuclei is shown in blue. *(from Campanella M. et al., 2009 Cell Press)*

Although the role of mitochondria in triggering cell death by initiating the complex signalling pathways of apoptosis is well defined , it is becoming clear that mitochondria could also accelerate progression towards necrotic cell death through the simple mechanism of ATP depletion due to ATPase activity during mitochondrial dysfunction. This process is limited by an endogenous inhibitor protein known as IF1 – the inhibitory factor of the F1Fo-ATPase. Since its discovery , a wealth of information has been gathered about the biochemical and molecular structure of this small protein, and yet it seems to have been remarkably neglected in more physiological studies. The protein inhibits ATPase activity in response to acidification of the mitochondrial matrix , which will usually accompany inhibition of mitochondrial respiration (i.e. during hypoxia/ischaemia) and in response to the reversal of F1Fo-ATP synthase activity to act as an ATPase [15]. Remarkably, it is known almost nothing about the relative expression levels of the protein in different tissues or cell types, or about the physiological impact of varied IF1 expression levels, or the mechanisms that regulate its expression. Currently, there are no animal models in which the gene is either over-expressed or knocked out; thus, the consequences of altered IF1 expression levels for cell or tissue function remain unknown.

Therefore, some recent investigations have set out to explore these issues by looking at the functional consequences of varying IF1 expression levels in cell lines. These data suggest that IF1 not only inhibits ATPase activity, and so protects cells from ATP depletion in response to hypoxia, but also IF1 appears to have a role in defining the conformation of the F1Fo -ATP synthase and mitochondrial cristae structure, as well as in regulating oxidative phosphorylation under normal physiological conditions.

In 1963, Pullman and Monroy [16] discovered the mitochondrial protein IF1 (inhibitor factor 1), encoded by the gene ATPIF1. IF1 binds to and inhibits the F1Fo-ATPase activity under conditions of both matrix acidification and ATP

hydrolysis. The mammalian ATPIF1 gene product contains 106–109 amino acids (depending on the species of origin), the first 25 amino acids represent a mitochondrial targeting presequence that is cleaved within the mitochondria to form the mature IF1 protein of 84 amino acids [17]. IF1 is highly conserved throughout evolution, with homologues found in birds, nematodes, yeasts and plants . This degree of conservation suggests that IF1 is a protein of major functional importance. Indeed, structure is sufficiently conserved such that IF1 from one species can inhibit F1Fo -ATPase from another, albeit with varying degrees of efficacy . It was recently suggested that IF1 might also localize to the plasma membrane where it is presumed to associate with an F1Fo-ATPase that has also been localized to the plasma membrane.

A calmodulin consensus binding motif is present in the middle of the IF1 protein , and it has been suggested that this motif might dictate its plasma membrane localisation in hepatocytes.

IF1-mediated F1Fo-ATPase inhibition is optimal at a pH of 6.7, a condition achieved in the mitochondrial matrix during severe ischaemia. The action of IF1 on F1Fo-ATP synthase activity, however, remains poorly documented in the literature. Given the requirement for an electrochemical potential, this partly reflects the technical difficulties involved in the study of F1Fo-ATP synthase activity in contrast with relatively straightforward measurements of ATP hydrolysis. Although some evidence suggests that IF1 can inhibit synthase activity, the importance of these observations remains unclear.

The detailed crystal structure of IF1-inhibited F1-ATPase has been solved, revealing two main features [18-19]. First, IF1 acts as a homodimer, simultaneously inhibiting two F1-ATPase units and, second, residues in the two protein complexes form numerous associations that involve several F1-ATPase subunits. Full association of IF1 with the F1Fo-ATPase is thought to occur only during ATP hydrolysis. Gledhillet al. suggest that low-affinity binding of IF1 to the surface of the F1 domain might occur even in the ground state; however, the functional consequence of this activity is not clear.

Dimerization of IF1 promotes dimerization of the F1-ATPase during ATP hydrolysis as demonstrated either using blue native gel electrophoresis or in

the IF1-inhibited F1-ATPase crystal structure. It has been suggested that dimerization of the IF1-inhibited ATPase structure could help to stabilize the complex against the torque induced by ATP hydrolysis in the F1 domain, or it might bring the F1-ATPase domains sufficiently close together (100 A˚) that they hinder each others' rotation. Dimerization of yeast F1Fo-ATP synthase occurs independently of IF1 [20] .

IF1 cell biology: functional consequences of altered expression

The functional consequences of genetic manipulation of IF1 protein levels were recently explored in cell lines (HeLa cells and muscle-derived C2C12 cells) [21], in which IF1 was either overexpressed by transient transfection or knocked down using small interfering RNA (siRNA).

Two approaches were used to assay IF1-mediated inhibition of F1Fo -ATPase activity: (i) measurements of the rate of ATP depletion after inhibition of oxidative phosphorylation and glycolysis (halting all ATP synthesis) to assess ATP hydrolysis by the F1Fo-ATPase; and (ii) measurements of $\Delta\psi_m$ in the face of inhibition of oxidative phosphorylation to assess the proton pumping activity of the F1Fo-ATPase.

In the first of these assays, cellular ATP synthesis was completely inhibited using either (i) iodoacetic acid (IAA) to inhibit glycolysis together with sodium cyanide (CN^-) to inhibit mitochondrial respiration, or (ii) IAA to inhibit glycolysis and oligomycin to inhibit oxidative phosphorylation. After inhibition of all cellular ATP synthesis, the rate of ATP depletion reflects the activity of all active ATP consuming processes in the cell. When oxidative phosphorylation is inhibited with CN^-, the F1Fo-ATPase activity contributes to the global rate of ATP consumption.

By contrast, when oxidative phosphorylation is inhibited with oligomycin, the F1Fo-ATPase activity cannot contribute to ATP consumption. The difference between the two rates therefore gives a measure of the specific contribution of

the F1Fo-ATPase as an ATP consumer. The concentration of free intracellular magnesium ($[Mg2+]_c$) increases as an index of ATP consumption as $Mg2+$ is released upon ATP hydrolysis. This provides a useful assay at the level of single cells, where direct measurements of [ATP] are not really practical [20].

After complete ATP depletion, cells underwent lysis; this occurred between 45 and 75 min in HeLa cells. In cells lacking IF1, the initial rate of ATP consumption was significantly faster in the presence of CN^- and IAA, and the time to lysis was significantly shorter compared with wild-type cells (grey versus black; Figure 2). In the presence of oligomycin and IAA, the rate of ATP consumption was slower and the time to lysis in wild-type cells was substantially delayed (red trace; Figure 2), indicating the overall ATP-consuming activity of the F1Fo -ATPase. Together, these experiments show that endogenous IF1 functionally inhibits ATPase activity in intact cells. Similar to the protection of rat cardiomyocytes against contracture, this experiment demonstrates that inhibition of F1Fo-ATPase activity is protective to cells. This is consistent with the finding that IF1 overexpression significantly reduced cell death in response to oxygen and glucose deprivation [22].

In a schematic cartoon (Figure 2b) we have illustrated the predicted impact of IF1 on changes in [ATP] and during the progression of a period of ischaemia. In cells with levels of IF1 sufficient to completely inhibit the ATPase activity (equivalent to the action of oligomycin), $\Delta\psi_m$ collapses rapidly as soon as the respiratory chain is inhibited, whereas [ATP] can be preserved for a considerable period of time until other ATP consumers drive ATP depletion. This timing will vary depending on the glycolytic capacity of the cell type and the activity of the ATP consumers. In marked contrast, in cells in which IF1 is absent, $\Delta\psi_m$ can be maintained at a new steady state for prolonged periods of time, but this occurs at the expense of cellular ATP, which becomes depleted more quickly. Once ATP is depleted, $\Delta\psi_m$ will collapse as there is no ATP left as a substrate for the F1Fo- ATPase [23].

These principles are readily established experimentally. Thus, CN^- inhibits electron transfer along the electron transport chain and hence its proton-pumping capacity, leading to depolarisation of mitochondria. Recently, the

extent of mitochondrial depolarisation in HeLa cells overexpressing IF1 was shown to be greater than that seen in wild-type cells. Conversely, when IF1 expression was suppressed, $\Delta\psi_m$ was maintained at a new steady state for prolonged periods of time. These experiments are more revealing than they might initially seem as they show that endogenous IF1 protein is not necessarily expressed with a fixed stoichiometry in relation to the F1Fo -ATP synthase. That activity can be increased or decreased by genetic manipulations argues that there is room for regulation of expression of this protein in relation to that of the F1Fo protein complex. This idea is strengthened by several observations. In central nervous system cultures containing both astrocytes and neurons, immunofluorescence measurements showed that ratios between the expression levels ofthe F1Fo-ATP synthase b-subunit and IF1 protein levels varied dramatically between the two cell types. Neurons,with a relatively low b-subunit:IF1 ratio, exhibited rapid loss of $\Delta\psi_m$ in response to CN^-, whereas astrocytes, with high b-subunit:IF1 ratio, maintained $\Delta\psi_m$, albeit at a reduced level [20].

F1Fo-ATPase activity was clearly required for the maintenance of $\Delta\psi_m$ because treatment of astrocytes with oligomycin caused rapid mitochondrial depolarization.

Reactive Oxygen Species

Reactive oxygen species (ROS) and the cellular redox state are increasingly thought to be responsible for affecting different biological signaling pathways. ROS are formed from the reduction of molecular oxygen or by oxidation of water to yield products such as superoxide anion ($O_2^{\bullet-}$), hydrogen peroxide (H_2O_2), and hydroxyl radical ($\bullet OH$).

In a biological system, the mitochondria and NAD(P)H oxidase are the major sources of ROS production. In moderate amounts, ROS are involved in a number of physiological processes that produce desired cellular responses.

However, large quantities of ROS in a biological system can lead to cellular damage of lipids, membranes, proteins,and DNA. Nitric oxide (NO•) is another contributor to ROS concentration and the formation of reactive nitrogen intermediates (RNIs). NO• is generated by specific nitric oxide synthases that also contribute to a large number of physiological processes. NO• can react with superoxide to form a potent oxidizing agent, peroxynitrite ($ONOO-$), which contributes to cellular damage and oxidative stress.

Oxidative stress results from overproduction of ROS and/or decreased system efficiency of scavengers such as vitamin C, vitamin E, and glutathione.

The direction of many cellular processes, such as phosphorylation and dephosphorylation and regulation of the cell cycle, can be determined by the redox state. Increases in ROS can lead to an imbalance of the cellular oxidation state, disrupting the redox balance. The intracellular ROS concentration can be estimated using the redox potential, E. A cell contains many biological redox couples, such as NADP+/NADPH and GSSG/2GSH, which allow the cell to maintain redox homeostasis. NADPH has the lowest reduction potential and thus serves as the driving force for other redox couples. GSSH/GSH is the main redox buffer of the cell and is found throughout all cellular compartments. The addition of oxidants to a cell system results in an increased [GSSG]/[GSH] ratio, thereby increasing the value of E above a specific threshold, which is representative of an oxidative state.

Mitochondria are major sources of reactive oxygen species; the main sites of superoxide radical production in the respiratory chain are Complexes III and I, with a general consensus that production at Complex I is about half of that at Complex III; however, other mitochondrial enzymes,such as Complex II, glycerol-1-phosphate dehydrogenase, and dihydroorotate dehydrogenase, are also involved in production of ROS.

ETC works basically with one-electron transfer steps and the redox centers present in oxphos complexes can potentially transfer electrons to molecular oxygen. ROS production in mitochondria depends mainly on both oxygen concentration and redox status of ETC complexes, and in physiological

conditions both parameters are actually determined by tissue metabolic requirements.

Since the structure of Complex I is not completely known, the site of electron leak has not been located and all major cofactors have been proposed as site of oxygen reduction: FMN, iron-sulfur clusters N2 and N1a and the semiquinone radical formed upon ubiquinone reduction [24-25]. However, the electron leak from one or more of these sites results in superoxide anion radicals (O2•-) production in the matrix.

One-electron reduction of oxygen in Complex III is accomplished by ubisemiquinone and increases in presence of antimycin, an inhibitor that binds one of the CoQ reduction sites; the release of superoxide anion from Complex III may occur on both side of inner membrane [26].

Anion superoxide production by Complex I reaches its maximal rate during reverse electron transfer (RET), wich occurs when electron supply, i.e. from succinate, reduces CoQ that in presence of a significant high ΔP could give electrons back to Complex I leading to formation of NADH from NAD+ through FMN; the role of Complex I in this process has been confirmed by use of rotenone. The RET-associated superoxide production is deeply dependent on ΔP since it could be completely abolished by even small decreases in the proton electrochemical potential achieved through addition of ADP or uncoupler [27].

Increase in Complex I prosthetic groups reduction may also occurs in presence of increased NADH/NAD+ ratio that may arise when respiratory chain activity is inhibited [28].

Thus, it is clear that alterations either in Complex I activity and structure or in the whole oxphos system might likely lead to an overproduction of ROS that could reflect in a non-reversible oxidative modification of lipids, proteins and nucleic acids. Although it has been demonstrated that inhibition threshold for Complex I (30%) or Complex III (70%) must be reached before to observe a significant ROS production, in a context of partial energetic impairment due to mutations in mtDNA genome also minimal shifts in the redox equilibrium might represent a further input of stress for the cell [28].

Because of the potential deleterious effect of a natural by-product of mitochondrial metabolism aerobic cells evolved efficient systems for ROS scavenging. The ROS-scavenging system must be highly regulated to rapidly answer to even slight changes in the redox state of cell. Since all genes implied in maintaining the correct balance between ROS production and scavenging are nuclear encoded, a proper mitochondria-nucleus cross-talk is of primary importance to counteract oxidative stress risk.

Superoxide dismutase catalyzes dismutation of superoxide anion in hydrogen peroxide. In mammalian three genes encoding superoxide dismutases with different localization have been found. SOD1 and SOD3 encode two enzymes containing copper and zinc in their catalytic site (CuZnSOD) but showing different localization: SOD1 product is localized in cytoplasm, nuclear compartments, mitochondrial intermembrane space and lysosomes of mammalian cells while SOD3 product exists as a homotetramer and is located in the extracellular environment. The expression pattern of SOD3 is highly restricted to specific cell type and tissues where its activity can exceed that of SOD1 and SOD2. A third isoform of SODs has manganese as a cofactor (MnSOD) and is localized in mitochondrial matrix of aerobic cells where it is active in the tetrameric form [29].

Glutathione peroxidase (GPX) contains selenium in the catalytic site and catalyzes reduction of hydrogen peroxide by glutathione; different isoforms are present in cytoplasm and mitochondria and are differently expressed depending on tissues [30].

Peroxiredoxins (Prdx) are thiol-dependent enzymes working as hydrogen peroxide scavenger; isoform 3 is exclusively localized in mitochondrial matrix.

Catalase catalyzes hydrogen peroxide conversion in H_2O and O_2, is a tetramer containing heme as prosthetic group and is localized in peroxisomes, in cytosol and in heart mitochondria [1].

Non-enzymatic systems like glutathione, thioredoxines and vitamins (E, C) which can participate to catalytic action of antioxidant enzymes as cofactors, are as well fundamental in maintaining the balance in the redox state of cells.

Intracellular ROS originate from multiple sites, including the mitochondrial electron transport chain, cytochrome P-450 oxygenase, xanthine oxidase (XO), lipoxygenase, cyclooxygenase, and uncoupled nitric oxide (NO) synthase (NOS). NADPH oxidase, a prominent source of ROS in vascular tissue, has several isoforms localized to different sites within the cell. NADPH oxidase that contains the NOX2 catalytic subunit can be plasmalemmal bound and produce $O_2\cdot$ extracellularly or within the cytosol. The extracellularly generated $O_2\cdot$ can reenter the cell through anion-selective chloride channel-3 channels or by conversion to H_2O_2 via extracellular SOD [31].

The NOX4 containing oxidase is located in endosomes , focal adhesions, and nuclei and generates $O_2\cdot$ intracellularly. Other members of the NOX family include NOX1, which can be found in various subcellular localizations such as nuclei and caveolae, NOX3 and NOX5, which both have been shown to colocalize with the plasma membrane.

Thus subcellular localization of NADPH oxidase allows for stereospecific release of $O_2\cdot$, which is spontaneously or catalytically (SOD) converted to H_2O_2, the primary signaling ROS. As an uncharged molecule, H_2O_2 can traverse cell membranes, is rapidly inactivated by endogenous catalase and peroxiredoxins, and can reversibly alter enzyme function through oxidative modification of susceptible residues, including arginine, cysteine, histidine, and others. These properties strongly support a signaling role for intermediate doses of H_2O_2. Signaling dose ranges for H_2O_2 were established in human and animal models and vary from 1 µM to 10 mM. Interestingly, in rat coronary arterioles, sensitivity to H_2O_2 is increased with aging [32].

2 Oxygen Sensing and Homeostasis

The survival of all metazoan organisms is dependent on the regulation of O2 delivery and utilization to maintain a balance between the generation of energy and production of potentially toxic oxidants.

About 1.5 billion years ago eukaryotic organisms appeared containing mitochondria, sub cellular organelles in which glucose is oxidized to carbon dioxide and water, thereby completing the energy cycle. Reducing equivalents are generated that pass through the mitochondrial respiratory complex, which results in the formation of a proton gradient that is used to drive the synthesis of adenosine 5′-triphosphate.

Humans have evolved complex circulatory, respiratory, and neuroendocrine systems to ensure that oxygen levels are precisely maintained, since an excess or deficiency may result in the death of cells, tissue, or the organism.

Oxygen homeostasis represents an organizing principle for understanding evolution, development, physiology, and disease. Historically, oxygen sensing was thought to be limited to specialized cells, such as the glomus cells of the carotid body, which depolarize within milliseconds in response to hyperoxia by means of incompletely understood mechanisms. We now recognize that all nucleated cells in the body sense and respond to hypoxia.

Under conditions of reduced oxygen availability, hypoxia-inducible factor 1 (HIF-1) regulates the expression of genes that mediate adaptive responses. In hypoxic cells, the transcription of several hundred messenger RNAs (mRNAs) is increased, and the expression of an equal number of mRNAs is decreased. The changes are dependent on HIF-1 in both cases, but HIF-1 binding is detected only at genes with increased expression. HIF-1 decreases mRNA expression indirectly by regulating transcriptional repressors and microRNAs.

HIF-1 was first identified in human cells as a regulator of erythropoietin, the hormone that controls red-cell production; vascular endothelial growth factor (VEGF), which stimulates angiogenesis; and glycolytic enzymes, which adapt cell metabolism to hypoxic conditions oxygen sensing, gene expression, and adaptive responses to hypoxia)[33].

Mechanism of HIF-1 Activation

Active HIF-1 is a heterodimer composed of a constitutively produced HIF-1β subunit, which is stable irrespective of the oxygen level, and a labile HIF-1α subunit. Canonically, it is assumed that regulation of HIF-1α is indeed the critical event implicated in the HIF-mediated cellular response to low oxygen, as HIF-1α is highly induced by hypoxia [33-34]. The HIF-1α subunit is virtually undetectable under normoxic conditions, since it is rapidly degraded by the ubiquitin–proteasome pathway.

Under normoxic conditions **(Fig 7A)**, HIF-1α has a very short half-life of less than 5 min, being continuously synthetized and degraded [35]. It is well established that under normal oxygen levels, HIF-1α is hydroxylated on proline residues 402 and 564 in the oxygen-dependent degradation domain by specific prolyl hydroxylases (PHDs) [36] that require oxygen and 2-oxoglutarate, as co-substrates, and iron (Fe2+) and ascorbate, as co-factors. The use of iron by these enzymes explains the hypoxia-mimetic effects of iron antagonists and chelators, such as desferrioxamine (DFO) and cobalt chloride [37].

Although 2-oxoglutarate, a tricarboxylic acid (TCA) cycle intermediate, is essential for the activity of PHDs because of its role in the coordination of iron in the catalytic core, other TCA cycle intermediates such as succinate and fumarate appear to inhibit PHDs by competing with 2-oxoglutarate for binding to the active site. Once hydroxylated, HIF-1α is recognised by the von Hippel–Lindau protein (VHL), which is part of an ubiquitin ligase complex known as E3 ligase complex that targets HIF-1α for polyubiquitination and subsequent proteasomal degradation. In addition to VHL, the E3 ligase complex is formed by the RING-finger protein RBX1, which is thought to recognise a cognate E2, as well as several adaptor proteins, such as elongin B, elongin C and cullin 2 [38]. The asparagine 803 residue of HIF-1α is also hydroxylated under normoxic conditions by a specific asparagine hydroxylase named factor-inhibiting HIF-1 (FIH-1), which impairs the interaction of the transcriptional co-activators p300/CREB binding protein (CBP) with the HIF-1α C-terminal

transactivation domain. This leads to further repression of the transcriptional activity of HIF-1. Like PHDs, FIH-1 requires 2-oxoglutarate, iron, ascorbate and dioxygen to induce hydroxylation; however, as opposed to PHDs, FIH-1 is not inhibited by intermediates of the TCA cycle.

When oxygen becomes limited (**Fig 7B)**, the proline residues are no longer hydroxylated and HIF-1α escapes degradation, accumulating in the cell. Subsequently, HIF-1α is translocated into the nucleus, where it dimerises with HIF-1β and binds to a core pentanucleotide sequence (5′-RCGTG-3′) in hypoxia-responsive elements of the promoter or enhancer sequences of target genes. Ultimately, HIF-1 activates the expression of numerous genes that help cells to survive at low oxygen levels. In addition, p300/CBP interact with HIF-1α, due to inhibition of Asn803 hydroxylation, increasing the transcriptional activity of HIF-1 [35].

Hypoxic responses are also mediated by HIF-2, a heterodimer composed of HIF-1β and HIF-2α (a paralogue of HIF-1α that is also regulated by oxygen-dependent hydroxylation). HIF-1α is present in all nucleated cells of all metazoan species, whereas HIF-2α expression is restricted to certain cell types within vertebrate species and plays an important role in both erythropoiesis and vascularization. Another paralogue, HIF-3α, appears to function as an inhibitor of HIF-1a [39].

Establishing the specific roles of HIF-1a, HIF-2a, and HIF-3a in oxygen homeostasis is a major challenge of current research [40].

HIF-1α$^{-/-}$ mouse embryos, which lack HIF-1α, are arrested in their development at midgestation and die from cardiac and vascular defects and decreased erythropoiesis, indicating that all three components of the circulatory system are dependent on HIF-1 for normal development.

PDH1 and PHD3 also hydroxylate HIF-1a when overexpressed, but their physiological functions have not been established. PHD2 activity is reduced under hypoxic conditions either as a result of substrate limitation or as a result of inhibition of the catalytic center [which contains Fe(II)] by ROS generated at complex III of the mitochondrial respiratory chain [41].

ROS levels increase in response to hyperoxia, but HIF-1a levels do not, which suggests that the site of ROS generation may be different in hyperoxic cells or that ROS generation by complex III is necessary, but not sufficient, to induce HIF-1a under hypoxic conditions. FIH-1 (factor inhibiting HIF-1) is another dioxygenase that hydroxylates asparagine residue 803 of HIF-1a and, thereby,blocks its interaction with the coactivator p300. The half-life of HIF-1a is also regulated in an O2-independent manner by the competitive binding of either heat shock protein HSP90, which stabilizes the protein, or RACK1, which interacts with Elongin C and, thereby, promotes HIF-1a ubiquitination and degradation that is independent of PHD2 and VHL . A second major O2-independent regulatory mechanismis the stimulation of HIF-1a protein synthesis by signal transduction via phosphatidylinositol 3-kinase, protein kinase B (AKT), and mammalian target of rapamycin [33].
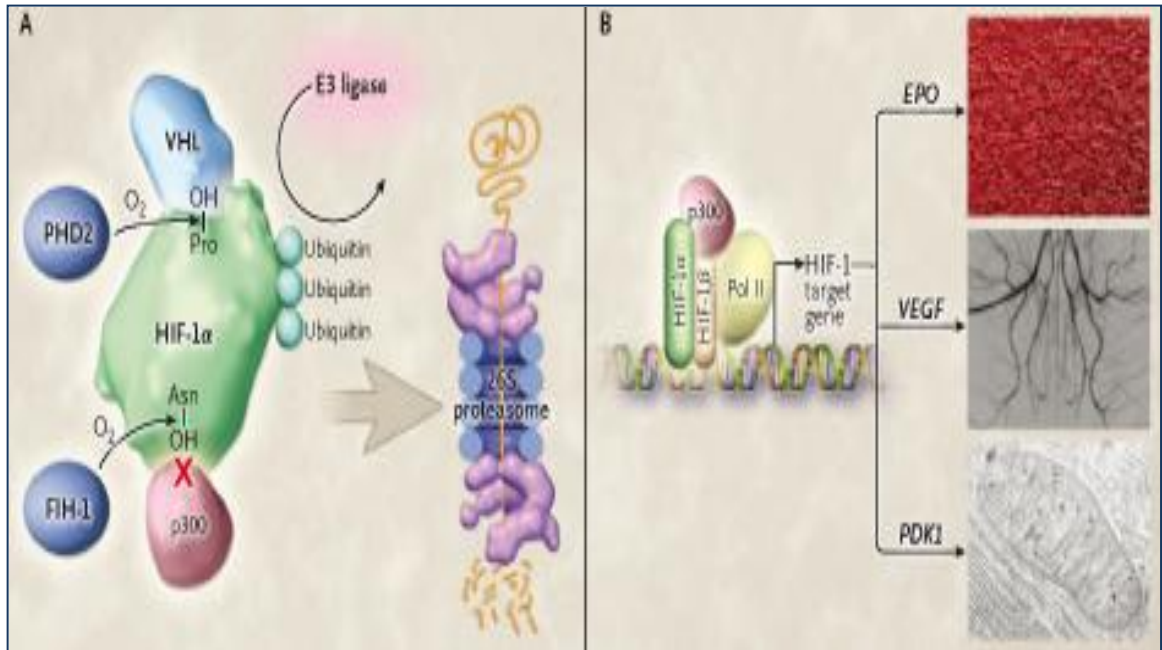
Figura 6. In well-oxygenated cells **(Panel A)**, prolyl hydroxylase domain 2 (PHD2) uses oxygen to hydroxylate hypoxia-inducible factor 1 (HIF-1α) on a proline residue (Pro–OH). The von Hippel–Lindau (VHL) protein binds to HIF-1α containing Pro–OH and recruits a ubiquitin E3 ligase. The polyubiquitination of HIF-1α flags the protein for degradation by the 26S proteasome. Factor inhibiting HIF-1 (FIH-1) also uses oxygen to hydroxylate HIF-1α on an asparagine residue (Asn–OH). HIF-1α containing Asn–OH cannot be bound by the coactivator protein p300, thereby preventing HIF-1α from activating gene transcription. Under hypoxic conditions **(Panel B)**, the Pro and Asn hydroxylation reactions are inhibited, and HIF-α (i.e., either HIF-1α or HIF-2α) rapidly accumulates, dimerizes with HIF-1β, recruits p300, binds to hypoxia response elements, and activates the transcription by RNA polymerase II (Pol II) of hundreds of target genes, such as the following: *EPO*, encoding erythropoietin(photomicrograph at top); *VEGF*, encoding vascular endothelial growth factor, (angiogram in middle); and *PDK1*, encoding pyruvate dehydrogenase kinase 1, which inhibits the conversion of pyruvate to acetyl coenzyme A for oxidation in the mitochondrion (electron micrograph at bottom). *(from Semenza GL., 2011 N. Engl. J Med)*

Regulation of cellular metabolism by HIF-1 α

Even the simple roundworm *Caenorhabditis elegans,* which consists of about 1000 cells and contains no specialized systems for oxygen delivery, expresses HIF-1, indicating that the primordial function of HIF-1 was to mediate adaptive responses that allow cells to survive oxygen deprivation. One way in which HIF-1 promotes cell survival under hypoxic conditions is by mediating a switch from oxidative to glycolytic metabolism. The glycolytic enzymes convert glucose to pyruvate, which can be converted either to acetyl coenzyme A

(CoA) for oxidation in the tricarboxylic acid cycle or to lactate as a glycolytic end product **(Fig. 8)**. HIF-1 activates the expression of lactate dehydrogenase A and pyruvate dehydrogenase kinase 1 (PDK1), thus tipping the balance from oxidative to glycolytic metabolism [39].
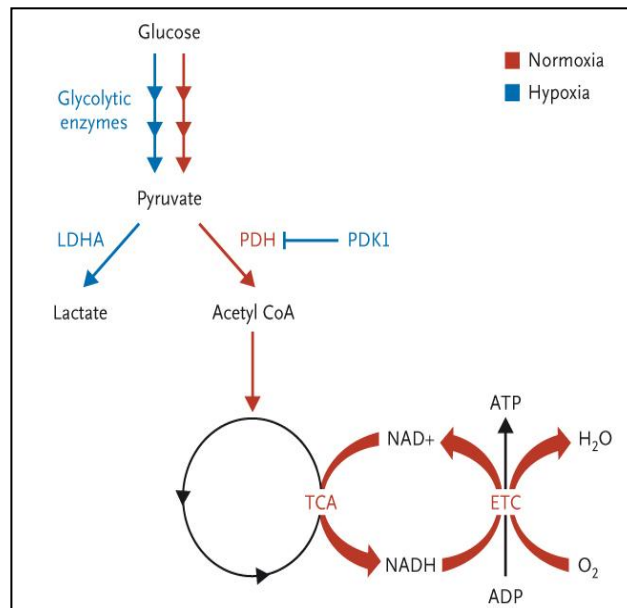

Figura 7. Regulation of Glucose Metabolism in Response to Changes in Cellular Oxygen Levels. Glucose is converted to pyruvate by the action of the glycolytic enzymes. In well-oxygenated cells (red pathway), pyruvate dehydrogenase (PDH) converts pyruvate to acetyl coenzyme A (CoA), which is oxidized in the mitochondrial tricarboxylic acid (TCA) cycle, generating electrons that are transported through a series of protein complexes (ETC) and are eventually transferred to oxygen to form water. The proton gradient established by the ETC is used to synthesize ATP. Under hypoxic conditions (blue pathway), pyruvate dehydrogenase kinase 1 (PDK1) inactivates PDH, and lactate dehydrogenase A (LDHA) converts pyruvate to lactate. The expression of the glycolytic enzymes is also induced to increase flux through the pathway

As compared with glycolysis, oxidative metabolism yields 18 times as much ATP per mole of glucose consumed. Although it is the conventional wisdom that cells respire until oxygen is depleted, at which point they switch to glycolysis, it is known that this model of metabolic regulation is incorrect. HIF-1α−/− fibroblasts are incapable of switching from oxidative to glycolytic metabolism when shifted from aerobic conditions of 95% air and 5% carbon

dioxide (20% oxygen, with a partial pressure of oxygen [PO2] of about 140 mm Hg) to hypoxic conditions (1% oxygen, with a PO2 of about 7 mm Hg).

ATP levels are higher in HIF-1α−/− cells at 1% oxygen than in HIF-1α+/+ cells at 20% oxygen, indicating that 1% oxygen does not limit ATP production. However, HIF-1α−/− fibroblasts maintained at 1% oxygen or less will die owing to toxic levels of reactive oxygen species [42].

HIF-1 plays three critical roles in the hypoxia-induced metabolic switch from oxidative to glycolytic metabolism. HIF-1 induces expression of: (1) upstream glucose transporters and glycolytic enzymes to increase flux from glucose to pyruvate; (2) PDK1 to block the conversion of pyruvate to acetyl CoA; and (3) lactate dehydrogenase A to convert pyruvate to lactate **(Fig 9)**.

Under aerobic conditions, electrons are transferred from NADH and flavin adenine dinucleotide (FADH2) (generated by oxidation of acetyl CoA) to mitochondrial complex I or II, then to complex III, and finally to complex IV, where they react with oxygen to form water. Under hypoxic conditions, the release of electrons is increased before the transfer to complex IV, resulting in the formation of superoxide, which is then converted to hydrogen peroxide and other toxic reactive oxygen species. Thus, there is sufficient oxygen for oxidative phosphorylation to occur in hypoxic fibroblasts, but at the cost of a loss of redox homeostasis [43].

The extent to which these findings apply to disease states, such as cancer and pulmonary hypertension, remains to be determined.
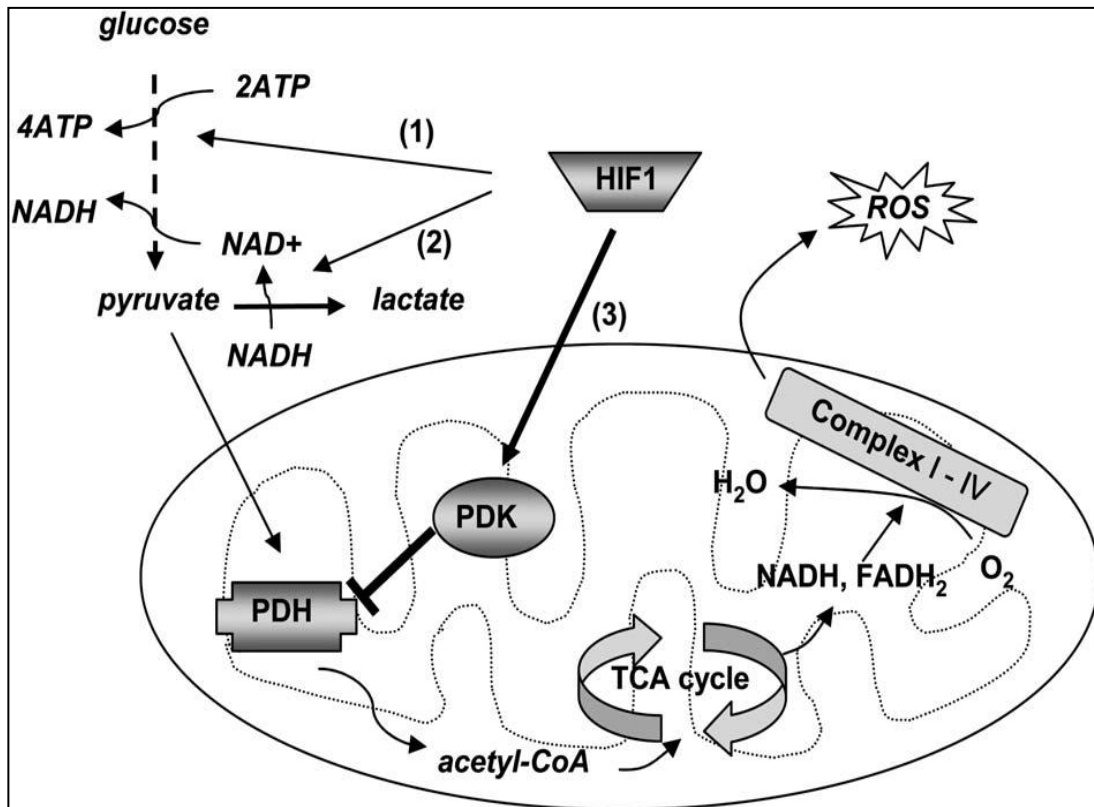
Figura 9. Regulation of hypoxia-induced metabolic switches by HIF-1. In hypoxic cells, HIF-1 stimulates increased glycolytic flux to pyruvate (1) and its reduction to lactate (2).In addition, HIF-1-induced PDK1 activity inhibits PDH (3), resulting in decreased flux through the TCA cycle. The resulting attenuation of oxidative phosphorylation is essential to prevent the generation of reactive oxygen species (ROS) resulting from ineffective electron transport under hypoxic conditions. HIF-1 mediates these effects through transcriptional activation of genes encoding glucosetransporters and glycolytic enzymes (1), lactate dehydrogenase A (2), and PDK1 (3). *(from Kim JW et al., Cell Metabolism, 2006)*

Effects of hypoxia on mitochondrial OXPHOS complexes

Oxygen is the terminal acceptor of electrons from cytochrome c oxidase, which has a very high affinity for it, being the oxygen concentration for half-maximal rate at pH 7.4 approxymately 0.7 µM [44].

It has been showed that the rate of O_2 consumption is not dependent on oxygen concentration up to 20 µM at pH 7.0. Thus, it has been found that the rate of O_2 consumption remained constant until $[O_2]$ fell below 15 µM [45]

Most reports in the literature consider hypoxic conditions occurring in cells at 5-0.5% O_2,

corresponding to a concentration of 46-4.6 µM in the cells culture medium.

During hypoxia, a number of changes on the OXPHOS machinery components, mostly mediated by HIF-1 have been found.

Kim et al., revealed that adaptation to hypoxia critically depends on the active inhibition of mitochondrial pyruvate metabolism and respiration.

HIF-1 actively suppresses metabolism through the tricarboxylic acid cycle (TCA) by directly trans-activating the gene encoding pyruvate dehydrogenase kinase 1 (PDK1). PDK1 inactivates the TCA cycle enzyme, pyruvate dehydrogenase (PDH), which converts pyruvate to acetyl-CoA. Forced PDK1 expression in hypoxic HIF-1a null cells increases ATP levels, attenuates hypoxic ROS generation, and rescues these cells from hypoxia-induced apoptosis. These studies reveal a hypoxia-induced metabolic switch that shunts glucose metabolites from the mitochondria to glycolysis to maintain ATP production and to prevent toxic ROS production **(Fig. 6).**

Moreover, HIF-1 is responsible of the regulation of COX activity. COX, which is located in the mitochondrial inner membrane, is a dimer in which each monomer consists of 13 subunits. Subunits I, II and III (COX1–COX3 respectively),which are encoded by the mitochondrial genome and constitute the catalytic core of the enzyme, are highly conserved in all eukaryotes. The high-resolution crystal structure of bovine COX revealed that subunit IV (COX4) interacts, via its transmembrane domain, with COX1 and, via its C-terminal hydrophilic domain, with COX2. COX4 binds ATP, leading to allosteric inhibition of COX activity at high ATP/ADP ratios.

Mammalian cells express a predominant COX4-1 isoform, whereas an alternative COX4-2 isoform is also expressed in certain tissues. However, neither the molecular mechanisms regulating expression of the COX4/1 and COX4/2 genes that encode these proteins, nor the functional significance of alternative isoforms, was known. Analysis of cultured mouse and human cells revealed that COX4-2 mRNA and protein expression were induced by hypoxia. HIF-1 heterodimers containing HIF-1β and either HIF-1α or HIF-2α bound to

hypoxia response elements located in the 5'-flanking region and first intron of the COX4/2 gene within nuclear chromatin of human cells cultured under hypoxic conditions [33].

Analysis of the effects of gain-of-function, loss-of-function and loss-of-function-with-subunit-rescue experiments for COX4-1 and COX4-2 revealed that the regulated expression of these subunits optimized the efficiency of respiration in human cells under aerobic and hypoxic conditions respectively [46].

When COX4-2 was replaced by COX4-1, there were significant decreases in O_2 consumption, COX activity and ATP concentration under hypoxic conditions. When COX4-2 replaced COX4-1 under non-hypoxic conditions, O_2 consumption, COX activity and ATP concentration were maintained at normal levels, but at the cost of increased ROS production and caspase activation.

Taken together, the results of these experiments indicate that the COX4 subunit switch constitutes a critical adaptive response of mammalian cells to hypoxia [33].

According with the evidence of Zhang et al., the respiration rate decrease has to be ascribed to mitochondrial autophagy, due to HIF-1-mediated expression of BNIP3. This interpretation is in line with preliminary results obtained by Solaini et al., where the assay of the citrate synthase activity of cells exposed to different oxygen tensions was performed and it indicated that the citrate synthase activity, which is taken as an index of the mitochondrial mass, and Oxygen levels are directly linked [44].

Zhang et al., found that mitochondrial autophagy is an adaptive metabolic response that promotes the survival of cells under conditions of prolonged hypoxia. This process requires the HIF-1-dependent induction of BNIP3 and the autophagy machinery as demonstrated by Beclin-1 and Atg5 loss-of function studies and the assessment of GFP-LC3 protein subcellular localization. Furthermore, they demonstrate that HIF-1 regulates mitochondrial mass under normal physiological conditions, as even partial deficiency of HIF-1 α had a profound effect on BNIP3 expression and mitochondrial mass in the lungs of mice exposed to room air [47].

Hypoxia alters the expression of hundreds of mRNAs required for many aspects of tumorigenesis, and the HIF transcription factors play a central role in this response.

Recently, the effect of hypoxia on microRNA expression was reported. microRNAs are a novel class of gene modulators that can each regulate as many as several hundred genes with spatial and temporal specificity. These non-coding RNAs have been proposed to contribute to oncogenesis by functioning either as tumor suppressors (e.g., miR-15a/miR16-1) or oncogenes (e.g., miR-155 and the miR-17-92 cluster).

Recently, it has been showed that moderate hypoxia decreases oxygen consumption and Complex I activity via the HIF-1-dependent upregulation of NDUFA4L2. This demonstrate that NDUFA4L2 is a HIF-1-dependent gene, emphasizing the role of HIF-1 in mitochondrial reprogramming and revealing NDUFA4L2 as an important element in metabolic adaptation to hypoxia.

PDKs could potentially cooperate with NDUFA4L2 to reduce mitochondrial Complex I activity under moderate hypoxic conditions, but it is also conceivable that NDUFA4L2 has other biological functions that cannot be accomplished by PDKs. For example, when metabolites that fuel the TCA cycle originate from pathways different from glycolysis (e.g., glutaminolysis or fatty acid oxidation), it would be necessary to reduce ETC activity in order to decrease mitochondrial function [48].

Hypoxia-induced NDUFA4L2 expression could fulfill this role, reducing oxygen consumption due to its strategic position downstream of the TCA cycle, possibly at Complex I. Likewise, hypoxia induces the upregulation of microRNA-210, which represses

ISCU1/2 [49-51]. These proteins facilitate the assembly of iron-sulfur clusters, including those in Complex I, Complex III, and aconitase, which are critical for electron transport and mitochondrial redox reactions. As a result, microRNA-210 represses mitochondrial respiration. In HeLa cells and in Human Umbilical Vein Endothelial Cells (HUVEC), ISCU1/2 protein does not decrease prior to 48 hr and only under 0.5% O2, while NDUFA4L2 becomes functional as early

as 24 hr at 1% O2. Moreover, ISCU1/2 recovery in hypoxic HeLa cells did not disturb proliferation. In summary [48].

As mentioned above in this thesis, the F1F0 ATPase (ATP synthase) is the enzyme responsible of catalysing ADP phosphorylation as the last step of OXPHOS. It is a rotary motor using the proton motive force across the mitochondrial inner membrane to drive the synthesis of ATP. It is a reversible enzyme with ATP synthesis or hydrolysis taking place in the F1 sector at the matrix side of the membrane, chemical catalysis being coupled to H+ transport through the transmembrane F0 sector. IF_1 protein binds to the catalytic F1 sector at low pH and low Δψm (such as it occurs in hypoxia/ischemia). IF1 appears to be associated with ROS production and mitochondrial autophagy (mitophagy). This is a mechanism involving the catabolic degradation of macromolecules and organelles via the lysosomal pathway that contributes to housekeeping and regenerate metabolites. Autophagic degradation is involved in the regulation of the ageing process and in several human diseases, such as myocardial ischemia/reperfusion, Alzheimer's Disease, Huntington diseases, and inflammatory diseases and, it promotes cell survival by reducing ROS and mtDNA damage under hypoxic conditions [44].

Campanella [20], reported that, in HeLa cells under normoxic conditions, basal autophagic activity varies in relation to the expression levels of IF1. Accordingly, cells overexpressing IF1 result in ROS production similar to controls, conversely cells in which IF1 expression is suppressed show an enhanced ROS production. In parallel, the latter cells show activation of the mitophagy pathway, therefore

suggesting that variations in IF1 expression level may play a significant role in defining two particularly important parameters in the context of the current review: rates of ROS generation and mitophagy.

Effects of hypoxia on mitochondrial structures and dynamics

Mitochondria form a highly dynamic tubular network, the morphology of which is regulated by frequent fission and fusion events [44].

In most cell types mitochondria form a reticular network or several such networks with additional solitary small tubular remnants, mostly resulting from fission of the central mitochondrial reticulum.

Electron tomography revealed details of the internal structure and established that cristae, visualized previously by 2 Delectron microscopy, represent sacks protruding deeply into the central matrix space of the mitochondrial tubules. Consequently, the major morphology features of a mitochondrion can be distinguished, such as the outer membrane (OM), topologically contouring the tubular surface; the inner membrane (IM), with its peripheral IM part termed inner boundary membrane (IBM) and intracristae parts (ICM); the intermembrane space, with its peripheral part (PIMS), located between OM and IBM, and the intracristae part (cristae sacks interiors, ICS); finally, the matrix filling the IM-engulfed space [52].

Apart from its role in filtering incoming molecules by porin/VDAC channels, the OM represents an external "information keyboard" or a "switchboard", where the integrative response of the BCL-family and other information proteins triggers induction or inhibition of various cellular processes, such as apoptosis, autophagy, and mitoptosis. At the OM, the information responses are also integrated with the activities of the major GTPase proteins, thereafter called mitodynamins, which dynamically affect shape-forming of the mitochondrial reticular network. In this way, mitodynamins specifically participate in cell death processes, whereas the BCL-family proteins BAX and BAK play a role in shaping of the mitochondrial network [52].

The fusion/fission machineries are modulated in response to changes in the metabolic conditions of the cell, therefore one should expect that hypoxia affect mitochondrial dynamics. Oxygen availability to cells decreases glucose oxidation, whereas oxygen shortage consumes glucose faster in an attempt to produce ATP via the less efficient anaerobic glycolysis to lactate (Pasteur

effect). Under these conditions, mitochondria are not fueled with substrates (acetyl-CoA and O2), inducing major changes of structure, function, and dynamics. However, the direct regulation of mitodynamins in the HIF pathway or hypoxic conditions has not been fully revealed as yet.

3 Diabetes

All forms of diabetes are characterized by hyperglycemia, a relative or absolute lack of insulin action, pathway-selective insulin resistance, and the development of diabetes-specific pathology in the retina, renal glomerulus, and peripheral nerve. Diabetes is also associated with accelerated atherosclerotic disease affecting arteries that supply the heart, brain, and lower extremities. In addition, diabetic cardiomyopathy is a major diabetic complication [53].

The majority of publications regarding the mechanisms underlying hyperglycemia-induced diabetic vascular damage focus on the 5 major mechanisms indicated above. However, the results of clinical studies in which only 1 of these pathways is blocked have been disappointing [54]. This led to that all 5 mechanisms are activated by a single upstream event: mitochondrial overproduction of the ROS.

1) **Increased Polyol Pathway Flux:** the polyol pathway is based on a family of aldo-keto reductase enzymes that can use as substrates a wide variety of carbonyl compounds and reduce these by NADPH to their respective sugar alcohols (polyols). It was first thought that glucose is converted to sorbitol by the enzyme aldose reductase, with sorbitol then oxidized to fructose by the enzyme sorbitol dehydrogenase (SDH), with NAD^+ as a cofactor. Several mechanisms have been proposed to explain how hyperglycemia-induced increases in polyol pathway flux could damage the tissues involved. The most cited is an increase in redox stress caused by the consumption of NADPH. Because NADPH is a cofactor required to regenerate reduced glutathione (GSH), and GSH is an important scavenger of ROS, this could induce or exacerbate intracellular oxidative stress [55].

2) **Increased Intracellular AGE (Advanced Glycation End products) Formation:** AGEs are formed by the nonenzymatic reaction of glucose and other glycating compounds derived from glucose and increased fatty acid

oxidation in arterial endothelial cells and most likely heart (eg, dicarbonyls such as 3-deoxyglucosone, methylglyoxal, and glyoxal) with proteins [56].

Intracellular production of AGE precursors can damage cells by 3 general mechanisms.

Firstly, intracellular proteins modified by AGEs have altered function. Secondly, extracellular matrix components modified by AGE precursors interact abnormally with other matrix components and with matrix receptors (integrins) that are expressed on the surface of cells. Finally, plasma proteins modified by AGE precursors bind to AGE receptors on cells such as macrophages, vascular endothelial cells, and vascular smooth muscle cells [57].

Clinically, diabetes is associated with poor outcomes following acute vascular occlusive events. Diabetic animals have a decreased vascular density following hindlimb ischemia and impaired wound healing. Human angiograms demonstrate fewer collateral vessels in diabetic patients compared with non diabetic controls. Clinically, this contributes to increased rates of lower limb amputation, heart failure, and increased mortality after ischemic events. These defects result in part from a failure to form adequate compensatory vasculogenesis in response to ischemia.

High glucose induces a decrease in transactivation by the transcription factor hypoxia-inducible factor (HIF)-1α, which mediates hypoxia-stimulated chemokine and vascular endothelial growth factor (VEGF) production by hypoxic tissue, as well as chemokine receptor and endothelial nitric oxide synthase (eNOS) expression in endothelial precursor cells in the bone marrow [53].

3) AGEs can signal through the cell surface receptor called "RAGE," which is a receptor for other non-AGE proinflammatory-related molecules as well. RAGE is highly conserved across species and expressed in a wide variety of tissues. It is up-regulated at sites of diseases such as atherosclerosis and Alzheimer . One of the main consequences of RAGE–ligand interaction is the production of intracellular ROS via the activation of an NADPH oxidase system. The ROS produced in turn activate the Ras–MAPK pathway, leading to activation of NF-

κB. Activation of NF-κB results in the transcriptional activation of many gene products, one of which is RAGE, as well as many others associated with diseases such as atherosclerosis [53].

4) **Increased Protein Kinase C Activation:** PKCs are a family of at least 11 isoforms that are widely distributed in mammalian tissues. The enzyme phosphorylates various target proteins. The activity of the classic isoforms is dependent on both Ca^{2+} ions and phosphatidylserine and is greatly enhanced by diacylglycerol (DAG). Persistent and excessive activation of several PKC isoforms operates as a third common pathway mediating tissue injury induced by diabetes-induced ROS [53]. Hyperglycemia primarily activates the β and δ isoforms of PKC in cultured vascular cells. In the diabetic retina, hyperglycemia persistently activates protein kinase C and p38α mitogen-activated protein kinase (MAPK) to increase the expression of a previously unknown target of PKC signaling, SHP-1 (Src homology-2 domain–containing phosphatase-1), a protein tyrosine phosphatase. This signaling cascade leads to platelet-derived growth factor (PDGF) receptor-β dephosphorylation and a reduction in downstream signaling from this receptor, resulting in pericyte apoptosis [58]. The same pathway, activated by increased fatty acid oxidation in insulin-resistant arterial endothelial cells and heart, may play an equally important role in diabetic atherosclerosis and cardiomyopathy. Over-activity of PKC has been implicated in the decreased NO production in smooth muscle cells, and has been shown to inhibit insulin-stimulated expression of eNOS in cultured endothelial cells. Activation of PKC by high glucose also induces expression of the permeability enhancing factor VEGF in vascular smooth muscle cells [59].

5) **Increased Hexosamine Pathway Flux:** Hyperglycemia and insulin resistance–induced excess fatty acid oxidation also appear to contribute to the pathogenesis of diabetic complications by increasing the flux of fructose 6-phophate into the hexosamine pathway. In this pathway, fructose 6-phosphate is diverted from glycolysis to provide substrate for the rate-limiting enzyme of this pathway, glutamine:fructose 6-phosphate amidotransferase (GFAT). GFAT converts fructose 6-phosphate to glucosamine 6-phosphate, which is

then converted to UDP-*N*Acetylglucosamine. Specific *O*-GlcNAc transferases use this for posttranslational modification of specific serine and threonine residues on cytoplasmic and nuclear proteins by *O*-GlcNAc. Inhibition of GFAT blocks hyperglycemia-induced increases in the transcription of both TGF-α and TGF-β. Although it is not entirely clear how increased flux through the hexosamine pathway mediates hyperglycemia-induced increases in the gene transcription of key genes such as TGF-α, TGF-β1, and PAI-1, it has been shown that hyperglycemia causes a 4-fold increase in *O*-GlcNAcylation of the transcription factor Sp1, which mediates hyperglycemia induced activation of the PAI-1 promoter in vascular smooth muscle cells and of TGF-β1 and PAI-1 in arterial endothelial cells [53].

ROS production in Diabetes

Oxidative stress is thought to be a major risk factor in the onset and progression of diabetes. Many of the common risk factors, such as obesity, increased age, and unhealthy eating habits, all contribute to an oxidative environment that may alter insulin sensitivity either by increasing insulin resistance or impairing glucose tolerance. The mechanisms by which this occurs are often multifactorial and quite complex, involving many cell signaling pathways. A common result of both types of diabetes is hyperglycemia, which in turn contributes to the progression and maintenance of an overall oxidative environment.

Macro- and micro-vascular complications are the leading cause of morbidity and mortality in diabetic patients, but the complications are tissue specific and result from similar mechanisms, with many being linked to oxidative stress. There is a large body of clinical evidence correlating diabetic complications with hyperglycemic levels and length of exposure to hyperglycemia. In **Fig 10** have been presented   principal sources of ROS production in diabetes mellitus. There are numerous data which demonstrate mitochondria ROS

overproduction (first of all superoxide) in diabetes and diabetic complications although it is difficult to identify the exact sites of ROS formation [60].

Disorder of physiological signaling functions of reactive oxygen species (ROS) superoxide and hydrogen peroxide and reactive nitrogen species (RNS) nitric oxide and peroxynitrite is an important feature of diabetes mellitus type 1 and type 2. It is now known that hyperglycemic conditions of cells are associated with the enhanced levels of ROS mainly generated by mitochondria and NADPH oxidase. It has been established that ROS stimulate many enzymatic cascades under normal physiological conditions, but hyperglycemia causes ROS overproduction and the deregulation of ROS signaling pathways initiating the development of diabetes mellitus.

High glucose (HG) can initiate the production of superoxide and hydrogen peroxide, precursors of reactive free radicals, which are able to stimulate the decline of antioxidant systems, directly damage many biomolecules, increase lipid peroxidation and develop the insulin resistance in diabetes. For example, Graier et al. proposed that HG can induce superoxide formation in aortic endothelial cells through metal-mediated oxidation. Du et al. showed that the incubation of human endothelial cells (HUVEC) with high glucose led to rapid increase in ROS formation, the activation of nuclear factor NFκB, the induction of apoptosis and NO synthase uncoupling by a glucose-specific mechanism. They also suggested that peroxynitrite can be a mediator of the cytotoxic effects of high glucose in endothelial cells [61].

Mitochondrial ROS have also been implicated in diabetic complications and progression of the underlying diabetic state; however, it is not clear whether mitochondria of diabetic origin really generate ROS independently of the surrounding diabetic milieu. Herlein et al. showed that the gastrocnemius, heart and liver mitochondria of streptozotocin diabetic rats were not irrevocably altered to produce excess superoxide either by complex I or complex III. Moreover, gastrocnemius and heart mitochondria demonstrated an increase and not decrease in respiratory coupling. In addition, mitochondria of insulin-deficient diabetic rats did show the signs of ROS overproduction [62].
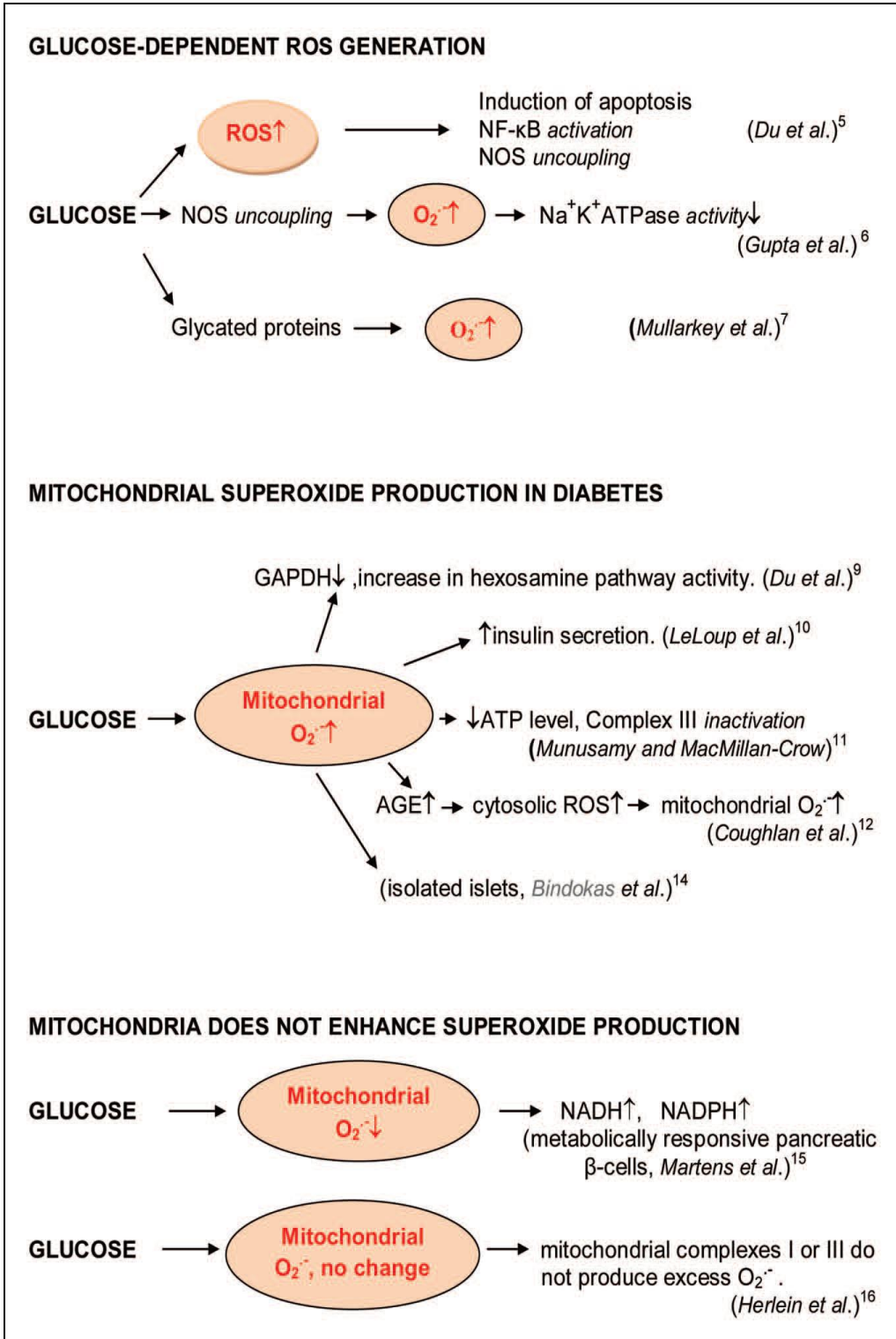
Fig 10. Induction of ROS formation by glucose in diabetes. Glucose enhanced ROS formation that induced apoptosis through the nuclear factor NFκB activation and NOS uncoupling in human endothelial cells.5 Hyperglycemia increased endothelial superoxide that impaired smooth muscle cell Na+-K+-ATPase activity.6 Glucose enhanced the formation of glycated proteins and superoxide formation.7

Mitochondrial superoxide production in diabetes. Glucose stimulated superoxide formation in diabetic mitochondria.9-12,14 Glucose decreased or was not changed mitochondrial superoxide formations.15,16. *(from Igor Afanas'ev, Oxidative Medicine and Cellular Longevity, 2010)*

Impairment of HIF-1α regulation in diabetes

Both hyperglycemia and hypoxia are important hallmarks of diabetic complications and appear to elicit several deleterious effects, leading to complications such as diabetic retinopathy, poor wound healing, neuropathies, cardiovascular and renal diseases. A feature that characterizes many of these complications is endothelial dysfunction mainly resulting from impaired ischemia-driven neovascularisation. It has consistently been observed that diabetic animals have decreased vascular density following hind limb ischemia and impaired wound healing [63]. Indeed, it has been extensively shown that ischemia induced production of eNOS, SDF-1, CXCR4, VEGF and other growth factors is decreased in diabetic tissues and in hyperglycemia [64].

In coronary heart disease, mRNA and protein levels of VEGF and its receptors VEGFR1 and VEGFR2 in the myocardium were found to be decreased by 40–70% both in diabetic rats and in insulin-resistant non-diabetic rats. Moreover, a twofold reduction in VEGF and VEGFR2 was observed in ventricles from diabetic patients compared with levels in ventricles from non-diabetic donors. In addition, decreased levels of VEGF in the renal glomeruli were correlated with podocyte cell death, diminished tissue repair and progression of renal disease in diabetic patients [65].

A number of independent reports have suggested that cellular adaptation to low oxygen is compromised in the presence of hyperglycemia, culminating in increased cell death and tissue dysfunction. For example, blood glucose levels showed a linear relationship with fatal outcome in response to an acute hypoxic challenge (i.e. acute myocardial infarction). It was further shown that AGEs, formed from dicarbonyls such as methylglyoxal, attenuate the angiogenic response in vitro, while in diabetic mice, inhibition of the formation of AGEs can restore ischemia induced angiogenesis in peripheral limbs [35].

Since HIF-1 is the master regulator of the cellular response to hypoxia, it is not surprising that HIF-1 deregulation is directly associated with the loss of cellular adaptation to low oxygen in diabetes. Indeed, there is a large body of evidence supporting this hypothesis and showing that HIF-1α is destabilized at low

oxygen levels by high glucose concentrations. It has been shown that high glucose decreases hypoxia-induced stabilization and function of HIF-1α in human dermal fibroblasts and human dermal microvascular endothelial cells in culture. This destabilization was not prevented by a prolyl hydroxylase inhibitor (ethyl 3,4-dihydroxybenzoate or EDBH), suggesting that other non-canonical mechanisms may be involved in the regulation of HIF-1α protein turnover in the presence of high glucose. In addition, HIF-1α production was found to be impaired during healing of large cutaneous wounds in young db/db mice and up-regulation of HIF-1α by gene-based therapy was shown to accelerate wound healing and angiogenesis in this model. Moreover, levels of HIF-1α were found to be decreased in biopsies from foot ulcers of diabetic patients as compared with venous ulcers that share the same hypoxic environment but are not exposed to hyperglycemia [66].

Downregulation of HIF-1 in response to hyperglycemia also appears to account for the decreased arteriogenic response triggered by myocardial ischemia in diabetic patients. In rats, myocardial infarct size increases in response to hyperglycemia and is associated with reduced production of the HIF-1α protein. As mentioned above, endothelial dysfunction in diabetes is related to impairment of hypoxia-induced production of eNOS, SDF-1, CXCR4 and VEGF. This impairment can presumably be ascribed to destabilization of HIF-1α, since overexpression of Hif-1α normalizes VEGF levels, improves development of myocardial capillary network and inhibits cardiomyocyte hypertrophy and cardiac fibrosis following myocardial injury [67]. In addition, increased expression or stabilization of HIF-1α is critical to improve wound healing [68] and it enhances the vascular response to critical limb ischemia in diabetic mice. This mechanism appears to involve an increase in limb perfusion and function, an increase in the number of circulating EPCs, vessel density and luminal area and a decrease in tissue necrosis [69].

Important findings include the observation that, compared with non-diabetic patients, patients with type 2 diabetes have decreased HIF-1β mRNA levels in pancreatic islets, suggesting that changes in the function of HIF-1 can contribute to the development of diabetes. A human HIF-1α genetic

polymorphism that results in P582S is associated both with type 2 diabetes [70] and the absence of coronary collaterals in patients with ischemic heart disease. These observations highlight a critical link between diabetes, the HIF-1 pathway and endothelial dysfunction.

Although the molecular mechanisms that underlie impairment of HIF-1 in diabetes remain poorly understood, some recent studies envision pathways whereby diabetes may lead to the downregulation of HIF-1. For example, Gurtner and collaborators reported two different mechanisms, both relying on the effect of increased availability of methylglyoxal [64, 71] in diabetes. Indeed, the authors showed that methylglyoxal modifies HIF-1α in hypoxic mouse dermal fibroblasts on two specific residues, arginine 17 and arginine 23, both of which belong to the basic helix-loophelix domain that is critical for the interaction with HIF-1β and formation of an active heterodimer. These modifications consistently reduced HIF-1 heterodimer formation and Glo1 (which encodes glyoxalase 1, the rate-limiting enzyme in the detoxification of methylglyoxale) overexpression prevented this impairment, emphasising the role of methylglyoxal in the loss of the cellular response to hypoxia in diabetes [64].

In a more recent study, it has been suggested that high glucose decreases the interaction between p300 and HIF-1α as a result of increased modification of p300 by methylglyoxal. Mutation of arginine 354 of p300 completely prevented high-glucose-induced methylglyoxal modification of p300 and restored the interaction with HIF-1α. The authors noted that methylglyoxal-induced modification of HIF-1α did not impair HIF-1α–p300 binding; however, a decrease in VEGF production was still observed, suggesting that impairment of associations between both HIF-1α–HIF-1β and HIF-1α–p300 might underlie the diabetes-induced defect in HIF-1 transcriptional activity. The authors further observed that the iron chelator Deferoxamine (DFO) improves HIF- 1α–p300 binding and augments HIF-1 activity and VEGF production at high glucose levels, by preventing p300 modification by methylglyoxal via a mechanism dependent on the decreased production of reactive oxygen species [71].

Dimethyloxalylglycine (DMOG), an oxoglutarate analogue known to be a potent inhibitor of PHDs, did not show the same effects as DFO, suggesting that DFO-induced effects are not likely to be dependent on PHDs and to influence HIF-1α protein stability. Alternatively, DFO appears to normalise the high glucose-induced defect in HIF-mediated transactivation, by a mechanism dependent on the decreased production of reactive oxygen species. The physiological significance of this mechanism is indicated by the observation that DFO enhances wound healing and neovascularisation in diabetic mice [71].

In a recent study, Bento and his group proposed a different mechanism for the regulation of HIF-1 under high glucose and hypoxic conditions, which also relies on methylglyoxal induced modifications. We showed that methylglyoxal is capable of inducing modifications on HIF-1α (such as the formation of methylglyoxal-derived hydroimidazolone 1, also referred to as MG-H1, adducts), leading to the increased association of HIF-1α with the molecular chaperones HSP40 and HSP70. These molecular chaperones subsequently recruit CHIP, which induces the polyubiquitination of HIF-1α and its degradation [72]. This mechanism of degradation appears to be mostly dependent on the proteasome, although other proteolytic pathways might also be involved in the degradation of methylglyoxal-modified HIF-1α. Canonically, CHIP has a key role in protein quality control by inducing ubiquitination of damaged proteins. The ability of CHIP to ubiquitinate HIF-1α under these conditions unravels an unanticipated role for CHIP in the loss of the cellular response to hypoxia under high glucose conditions such as diabetes. Interestingly, CHIP was also found to induce HIF-1α proteasomal degradation by a mechanism dependent on HSP70 in response to prolonged hypoxia [73].

Results and Discussion

1 Mitochondrial bioenergetics at low oxygen levels

Aim

Mitochondria are small organules with a central role in energy supply in cells, ROS production and apoptosis. Mitochondria have been implicated in several human disease and mitochondrial dysfunctions in hypoxia have been related with disorders like Type II Diabetes, Alzheimer Disease, inflammation, cancer and ischaemia/reperfusion in heart.

When oxygen availability becomes limiting in cells, mitochondrial functions are modulated to allow biologic adaptation. Different mitochondrial responses reported in literature depend on the degree of hypoxia, the duration of exposure, and the type of cells. The fine regulation of mitochondrial function has proved to be an essential metabolic adaptation to fluctuations in oxygen availability.

Cells exposed to a reduced oxygen concentration readily respond by adaptive mechanisms to maintain the physiological ATP/ADP ratio, essential for their functions and survival. In the beginning, the AMP-activated protein kinase (AMPK) pathway is activated [74], but the responsiveness to prolonged hypoxia requires the stimulation of hypoxia-inducible factors (HIFs).

HIFs are master transcription factors regulated in an O2-dependent manner by a family of prolyl hydroxylases (PHDs), which use O2 as a substrate to hydroxylate HIF-a subunits in conditions of normoxia [41]. These hydroxylated substrates are then ubiquitinated after recognition by VHL, and they are degraded by the proteasome. By contrast, PHD activity is inhibited in hypoxic conditions, and accordingly, HIF-α subunits accumulate, heterodimerize with HIF-β, and activate the expression of HIF-dependent target genes [75-76].

80-90% of oxygen in cells is consumed by mitochondrial respiration and in hypoxic conditions, the enzymes involved in oxidative phosphorylation

(OXPHOS), are supposed to be down-regulated. It has been shown that the mitochondrial respiration rate of cells exposed to a hypoxic environment was decreased but the molecular mechanism is still unclear. More recently, it has been reported that activation of HIF-1α induces pyruvate dehydrogenase kinase, which inhibits pyruvate dehydrogenase, suggesting that respiration is in fact decreased by substrate limitation [77]. Other reports have suggested that oxygen utilization is shifted in cells exposed to low O_2 levels due to nitric oxide (NO) inhibition of cytochrome c oxidase [78].

In this thesis we report a study of the mitochondrial bioenergetics of primary cells exposed to a prolonged hypoxic period . To shine light on this issue we examined the bioenergetics of fibroblast mitochondria cultured in hypoxic atmospheres (1% O_2) for 72 hours. Here we report on the mitochondrial organization in cells and on their contribution to the cellular energy state.

Growth of primary Human Dermal Fibroblasts at different oxygen tension

In this experiment we compared the cellular growth in fibroblasts cultured in 5mM glucose and exposed at different oxygen tension (from 21% to 0.5%).

As shown in figure 1 (left), the difference in oxygen levels does not significantly affect the growth, it means that the cell growth is not dependent on the oxygen tension. We hypothesized that this was due to the ability, of the cells cultured in different conditions, to maintain the same ATP availability. We measured the intracellular ATP content (figure 11 right) and we found a decrease of maximum 20% at 0.5% O_2. During hypoxia, ATP content does not change significantly since glycolysis becomes the main source of ATP.
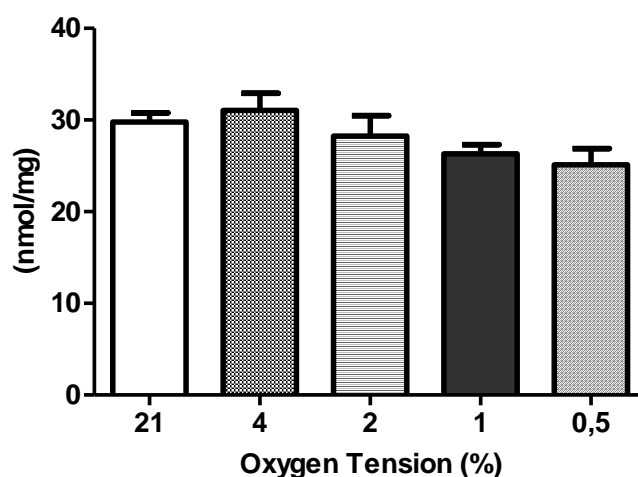
figure 1. **(left)** Growth of fibroblasts cultured in 5mM glucose for 72 hours at different oxygen concentrations. **(right)** Intracellular ATP content at different experimental conditions. Data are shown as average ± SD of three in-dependent experiments.

Oxidative phosphorylation and mitochondrial mass in hypoxia

Mitochondrial function has been evaluated in fibroblasts cultured in 5mM glucose at 21% O_2 and 1% O_2 for 72 hours . ATP synthesis rate has been considered as parameter for testing the effect of hypoxia on OXPHOS, it means on cellular energetic capability.

We measured Complex I-driven ATP synthesis in digitonin-permeabilized cells and in the presence of malonate, an inhibitor of succinate dehydrogenase complex. After inducing the *in vitro* ATP synthesis for 3 minutes, ATP extracted from samples was quantified with a chemiluminescent method based on luciferin-luciferase reaction using a known amount of ATP as standard.

As shown in figure 2 (left panel), cells exposed to 1% oxygen are characterized by a reduced capability (60%) to synthesize ATP in presence of Complex I substrates. Since when we measured the citrate synthase activity (figure 2-right panel),we found a decrease in mitochondrial mass, we explained the reduction in ATP synthesis is due to the decrease of number of mitochondria. In figure 3, the ATP synthesis rate values have been reported after normalization to citrate synthase activity of each analyzed sample. We

can conclude that most of the reduction in OXPHOS capability is due to the reduction of mitochondrial mass.
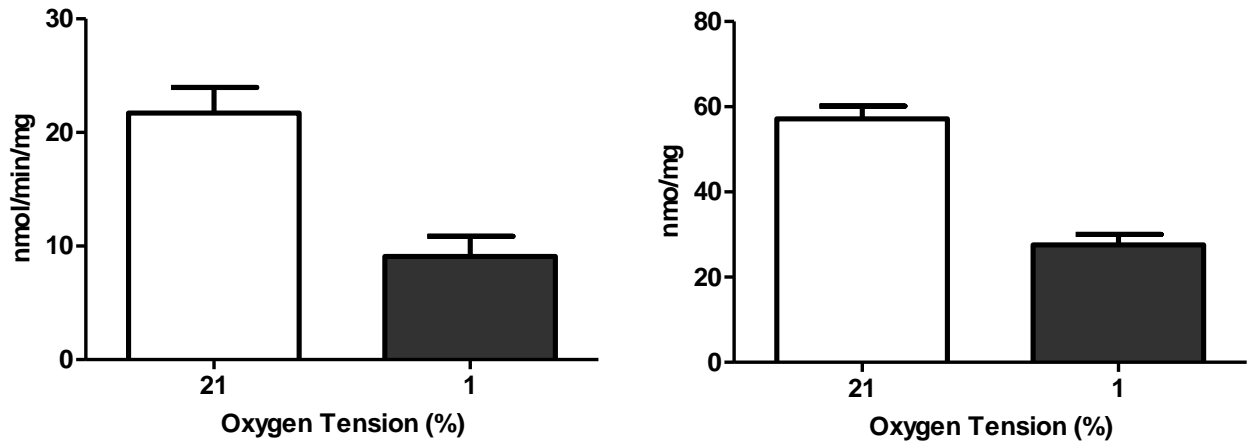

figure 12. Complex I-driven ATP synthesis rate (left panel), ATP synthesis rate in presence of NADH-dependent substrates. **Citrate Synthase activity** (right panel).
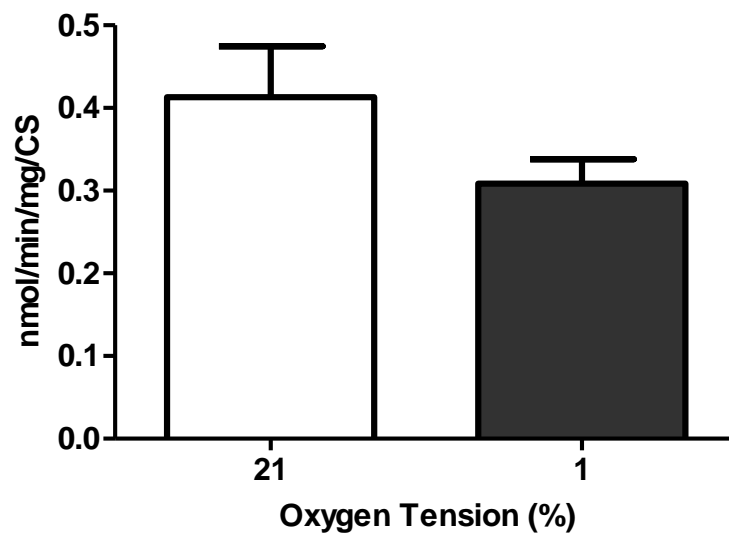

figure 3. **ATP synthesis rate,** ATP synthesis rate in presence of NADH-dependent substrates in fibroblasts cultured at 21% and 1% O_2. Values were normalized by citrate synthase activity considered as index of mitochondrial mass

Peroxides in Fibroblasts grown in Hypoxia

We compared the peroxide levels in fibroblasts grown for 72 h either at 21% and 1% O_2 tension . 21% O_2 induced the highest DCF fluorescence, corresponding to the highest level of peroxides; even though, prolonged hypoxia resulted in reduced peroxide levels (Figure 4). However, the peroxide levels decreased in hypoxia, suggesting that the reduction of mitochondrial mass has a main role in decreasing ROS producton in hypoxia.
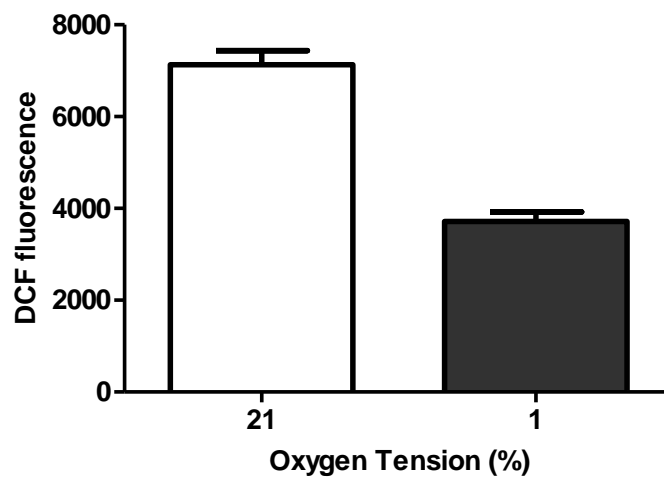

figure 4. ROS production in intact fibroblasts grown for 72 h in different experimental conditions. Reactive species were evaluated by measuring DCF fluorescence in cells cultured under normoxic (21% O_2) or hypoxic (1% O_2) conditions.

OXPHOS complexes in hypoxia exposed-fibroblasts

After the normalization of the OXPHOS rate versus the mitochondrial mass we wanted to estimate the level of the OXPHOS complexes to clarify how hypoxia affects the OXPHOS rate. Figure 5 shows a significant decrease of porin, the protein taken as an index of the mitochondrial mass, and a decrease of the OXPHOS complexes I, III, and IV levels in fibroblasts exposed to hypoxia.
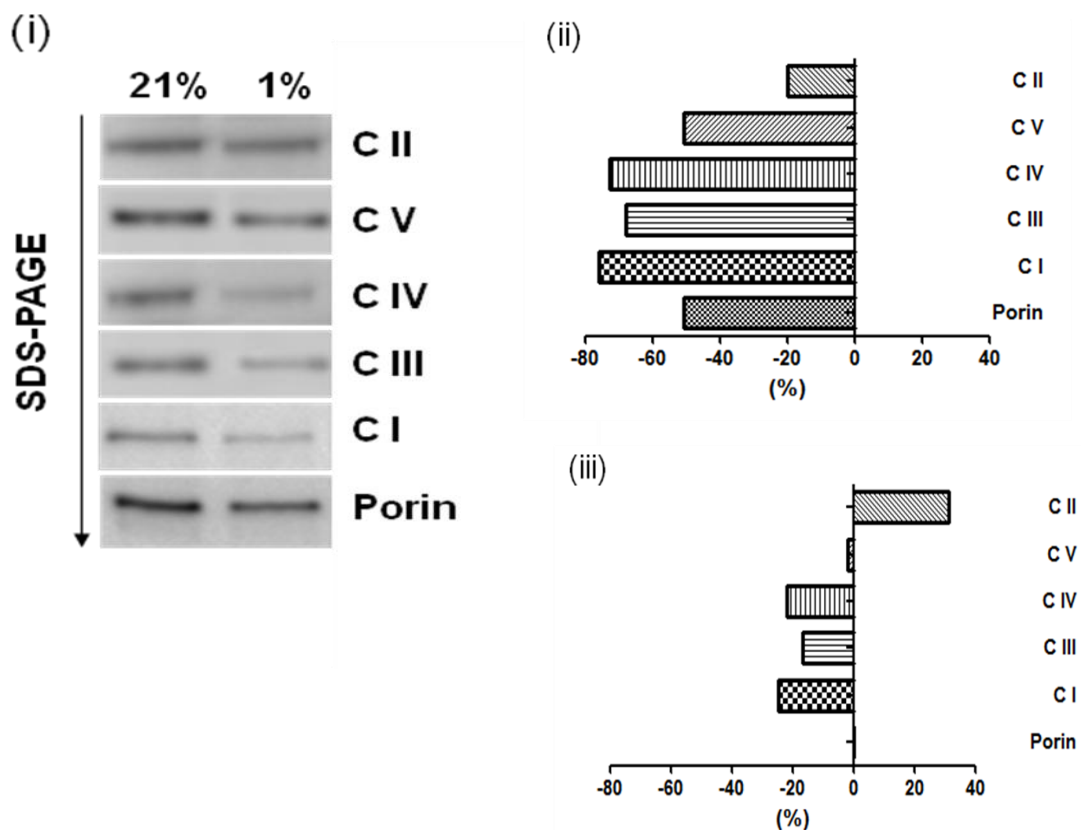

Figure 5. Immunodetection of OXPHOS complexes after SDS-PAGE separation Electrophoretic separation of cell lysates obtained from fibroblasts grown for 72 h in 5 mM Glucose (i); images have been quantified by QuantityOne Software and hypoxia was compared versus normoxia (ii); data were normalized on porin control, taken as internal standard (iii).

Discussion

Mammalian cells are able to sense decreased oxygen availability and activate adaptational responses including transcriptional activation of several hypoxia-inducible genes: erythropoietin, vascular endothelial growth factor, glycolytic enzymes, and glucose transporters. This allows increased O_2 delivery through enhanced erythropoiesis, angiogenesis and metabolic adaptations that facilitate glycolytic ATP production. Hypoxia-inducible factor 1 (HIF-1) is a heterodimeric transcription factor that regulates transcriptional activation of several genes responsive to the lack of oxygen, including erythropoietin, vascular endothelial growth factor, glycolytic enzymes, and glucose transporters.

The mechanisms of sensing low oxygen and transducing this signal to activate HIF-1 are not well understood. A role for a putative oxygen sensor molecule has been suggested. Another model proposes that the process of sensing decreased oxygen concentration involves NADPH oxidase activity. A decrease in available oxygen would result in decreased reactive oxygen species formation by NADPH oxidase, and this in turn would activate pathway(s) leading to HIF-1 induction [79]. Recently, a different model based on the role of the mitochondrial electron transport chain in hypoxia sensing was suggested . Inhibition of complex I and complex III of mitochondrial respiratory chain blocked HIF-1 DNA binding activity and expression of HIF-1 target genes in Hep3B cells under hypoxic conditions. In addition to hypoxia, several growth factors can activate HIF-1 and its target genes via different signaling pathways [80].

In 1998 Chandel [81] suggested that mitochondria may play a wider role in the functional responses of eukaryotic cells to changes in O2 concentration.

On the base of the studies reported, we evaluated how mitochondria are involved in the adaption to hypoxia.

The first evidence provided in this thesis is that long term hypoxia does not induce death of primary human fibroblasts. Previous studies showed that when

cells are exposed to hypoxia, glycolysis is stimulated and it can compensate the reduction of ATP production by oxidative phosphorilation [82].

Our data show that, despite ATP synthesis rate is reduced when oxygen availability decreases, the exposure of fibroblast to any oxygen level (4%, 2%,1%,0.5%) do not significantly affect the total ATP content, which is quite the same level of normoxia. These data might confirm the hypothesis reported above, that cells respond to lowered oxygen tension by increasing the amount of glycolytic enzymes and glucose transporters via the well-characterized hypoxia-inducible factor-1 (HIF). However, HIF is also responsible for the overexpression of lactate dehydrogenase (LDH), wich converts pyruvate in lactate with concomitant production of NAD^+, which is used in glycolysis. HIF also upregulates pyruvate dehydrogenase kinase 1 (PDK1), that inhibits the pyruvate dehydrogenase (PDH) decreasing TCA cycle and consequently oxidative phosphorylation in mitochondria.

The decrease of mitochondrial mass at 1% of oxygen explains the reduction of the ATP synthesis rate, that might be due, as reported by Thomas R.L. et al., 2011 [83], to the activation of mitochondrial autophagy, a mechanism involving the catabolic degradation of macromolecules and organelles in order to regenerate metabolites and promotes survival by reducing radical oxygen species (ROS) and DNA damage under hypoxic conditions.

The normalization of the ATP synthesis rate on citrate synthase activity highlighted that the decrease in ATP synthesis rate at 1% oxygen is not only due to a reduction in the number of mitochondria but it can occur through a different mechanism, linked to a dysfunction of mitochondrial complexes. From the quantitative analysis of the OXPHOS complexes by western blot, we can conclude that cells exposed to 1% O_2 are characterized by a reduction in the quantity of each complex, especially complex I, III, IV.

The role of oxidative stress in cells and tissues exposed to hypoxia is controversial, and the direct measurement of the effect of hypoxia on oxidative stress in human tissues has not been deeply understood under conditions of prolonged exposition to moderate hypoxia. Several studies support the hypothesis that hypoxia reduces ROS production in mitochondria since it

decreases mitochondrial respiration, others suggested that hypoxia increases ROS production because of its role in stabilize HIF.

In our hands, our data show that ROS level decrease in hypoxia as results of the reduction of oxidative phosphorylation activity in mitochondria and of mitochondrial mass.

Our results indicate that prolonged hypoxia cause a significant reduction of mitochondrial mass and of the quantity of the oxidative phosphorylation complexes. Thus, hypoxia is also responsible to damage mitochondrial complexes as shown after normalization versus citrate synthase activity.

This study demonstrated that to promote adaption and their survival, cells need to change their metabolism when are exposed to a crisis status, like hypoxia.

It is important to understand how cells try to adapt to hypoxia and which pathways are involved and also the role of mitochondria in it, the biochemical mechanisms in order to define possible therapeutic targets.

A better understanding of the mechanism at the base of the adaption to hypoxia is useful to help in studying a lot of important pathologies in which the lack of oxygen is a common issue, such as heart ischemia, cancer, and diabetic complications.

2 Modulation of mitochondrial structure and function in hypoxia and hyperglycemia

Aim

Chronic complications of diabetes (retinopathy, nephropathy, neuropathy, and diabetes-accelerated arteriosclerosis) represent a major medical and economical concern.

All forms of diabetes are characterized by chronic hyperglycemia and the development of diabetes-specific microvascular pathology in the retina, renal glomerulus and peripheral nerve. As a consequence of its microvascular pathology, diabetes is a leading cause of blindness, end stage renal disease and a variety of debilitation neuropathies. Diabetes is also associated with accelerated atherosclerotic macrovascular disease affecting arteries that supply the heart, brain and lower extremities. As a result, patients with diabetes have a much higher risk of myocardial infarction, stroke and limb amputation [84].

The worldwide incidence of diabetes is set to rise dramatically from the present incidence of 150 million to an estimated 300 million in 2025 and assorted complications affecting the vascular system, kidney, and peripheral nerves are common and extremely costly in terms of longevity and quality of life [68].

The vast majority of publications about the mechanisms underlying hyperglycemia-induced diabetic vascular damage, focus on five major mechanisms: increased flux of glucose and other sugars through the polyol pathway, increased intracellular formation of advanced glycation end-products (AGEs), increased expression of the receptor for advanced glycation end-products and its activating ligands, activation of protein kinase C (PKC) isoforms, and overactivity of the hexosamine pathway. In 2000 was hypothesized that all five mechanisms are activated by a single upstream

event: mitochondrial overproduction of the reactive oxygen species (ROS) [53].

It is well established that hyperglycemia elicits an increase in reactive oxygen species (ROS) production, due to increased input of reducing equivalents into the mitochondrial electron transport chain [85]. The pathogenesis of chronic ulcers in diabetes is still unclear. A critical stimulus for normal wound healing is relative hypoxia and an impaired reaction to hypoxia could contribute to impaired wound healing. Under hypoxic conditions, HIF-1α is stabilized against degradation and transactivates and up-regulates a series of genes that enable cells to adapt to reduced oxygen availability.

HIF-1α plays a pivotal role in wound healing, and its expression in the multistage process of normal wound healing has been well characterized, it is necessary for cell motility, expression of angiogenic growth factor and recruitment of endothelial progenitor cells [86].

Catrina et al., [66, 87] have shown that hyperglycemia impairs HIF-1α stability and function.

ROS and HIF are strictly related, and several mechanisms are activated by HIF to contribute to the reduction of the ROS production in hypoxia. HIF can activate autophagy (mitophagy) by inducing BNIP3 and by this mechanism reduces the amount of ROS-producing organelles [47].

Physiological hypoxia induces a COX4-1 to COX4-2 subunit switch, an effect mediated by HIF-1 that is thought to optimize the efficiency of respiration during conditions of reduced oxygen availability [46].

Tello et al. [48], proved that mitochondrial Complex I activity is controlled by NDUFA4L2 during hypoxia and its induction during hypoxia helps keep intracellular ROS production in check, consistent with the fact that NDUFA4L2 limits Complex I activity and prevents increases in membrane potential.

Another effect of HIF on ROS production and mitochondria is the activation of pyruvate dehydrogenase (PDH) kinase 1 (PDK1), which phosphorylates and inactivates in its turn the catalytic subunit of PDH, the enzyme that converts pyruvate to acetyl coenzyme A. In this way it prevents the entry of pyruvate into tricarboxylic acid (TCA) cycle and by this decreases the flux through

electron transport counteracting the reduced efficiency of electron transport in hypoxia that would produce excessive ROS.

Catrina et al. [66], demonstrated that hyperglycemia impairs HIF-1α stability and function and has been suggested that by this it contributes to the development of chronic complications of diabetes (wound healing, coronary heart disease, nephropathy, etc.).

The results reported in this dissertation have been obtained at Rolf Luft Research Center for Diabetes, Karolinska Institutet in Stockholm and derive from a project focused on the study of the modulation of mitochondria structure and function induced by hypoxia and hyperglycemia and on prove the role of HIF-1α destabilization in the increase of ROS production by mitochondria. Our hypothesis was that HIF-1α destabilization induced by hyperglycemia is responsible of the increase of ROS production during hypoxia.

We therefore studied the effect of hyperglycemia and hypoxia on human dermal fibroblasts (HDFs) and human dermal microvascular endothelial cells (HDMECs) that were grown in high glucose, low glucose concentrations and mannitol as control for the osmotic challenge. Cells were cultured in normoxia (21% O_2) and hypoxia (1% O_2).

High glucose and hypoxia increases ROS production in HDFs and HDMEC

In order to investigate ROS production induced by hyperglycemia and or/hypoxia, HDFs and HDMEC cells were cultured in 5 mM glucose, 30 mM glucose and 30 mM mannitol and were incubated either in hypoxia chamber (1% O_2) and normoxia (21% O_2) for 18 hours. After the incubation cells were analyzed by flow cytometry. We used the carboxy-methyl-H2DCFDA probe that loses the acetate groups when cleaved by esterases after cell entry, leading to intracellular trapping of the non-fluorescent 2', 7'dichlorofluorescein. It is a widely used probe for its ability to detect a wide spectra of ROS that induce   its   subsequent   oxidation,   to   the   highly   fluorescent   product

dichlorofluorescein. For evaluating mitochondrial ROS, we use the MItosox Red probe, that permeates live cells where it selectively targets mitochondria. It is rapidly oxidized by superoxide but not by other reactive oxygen species (ROS) and reactive nitrogen species (RNS).

Interestingly, in contrast with the studies presented, here we show that in normoxia, both in HDFs and HDMEC high glucose does not induce ROS production as shown in figure 16. CM-DCFDA and Mitosox Red fluorescences did not present any difference between high glucose and low glucose exposed-cells. Indeed, the combination of hypoxia and hyperglycemia for 18 hours induced an increase in ROS production, which has been pointed out by the high fluorescence of both DCFDA and Mitosox Red, either in HDFs or HDMEC.
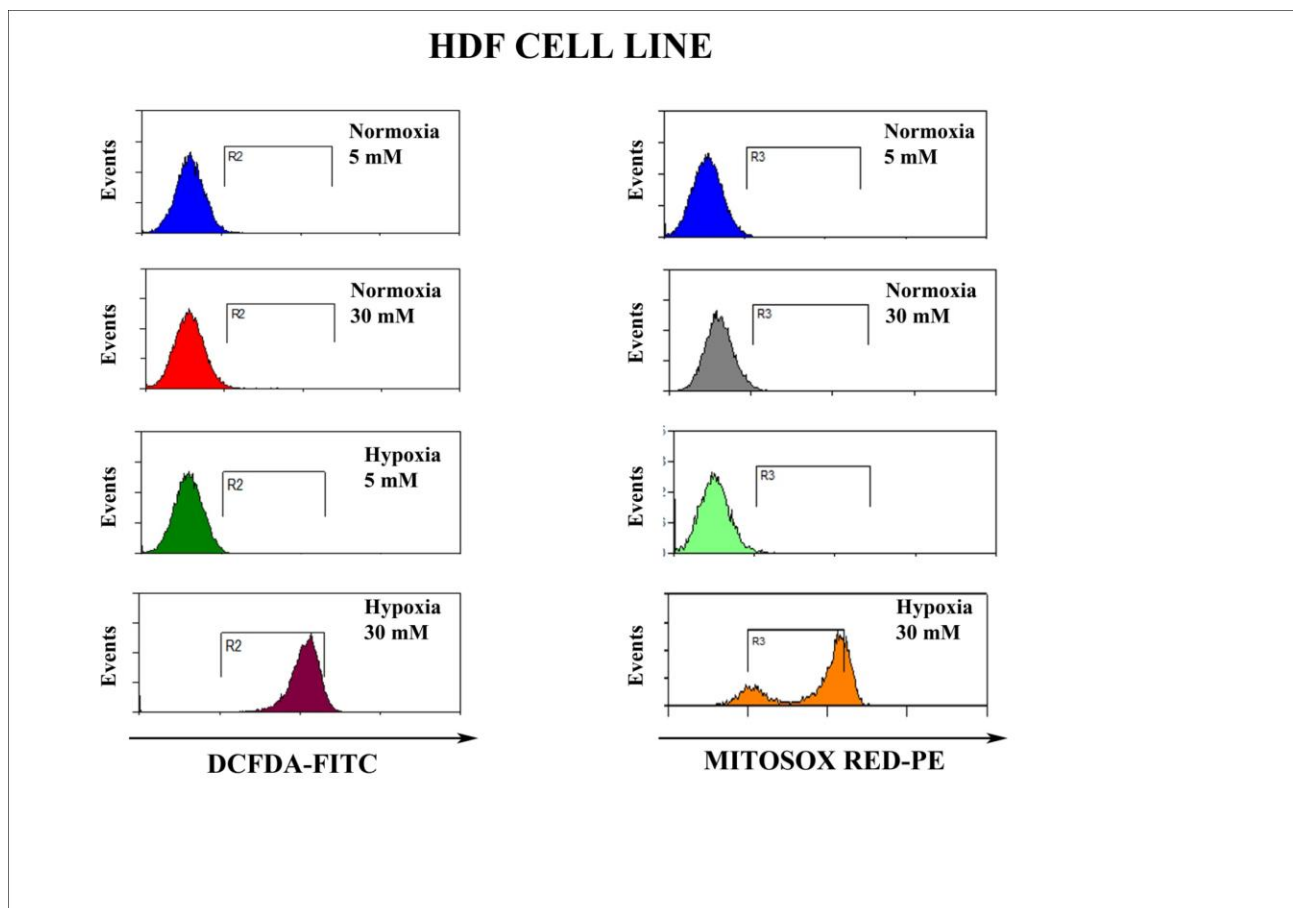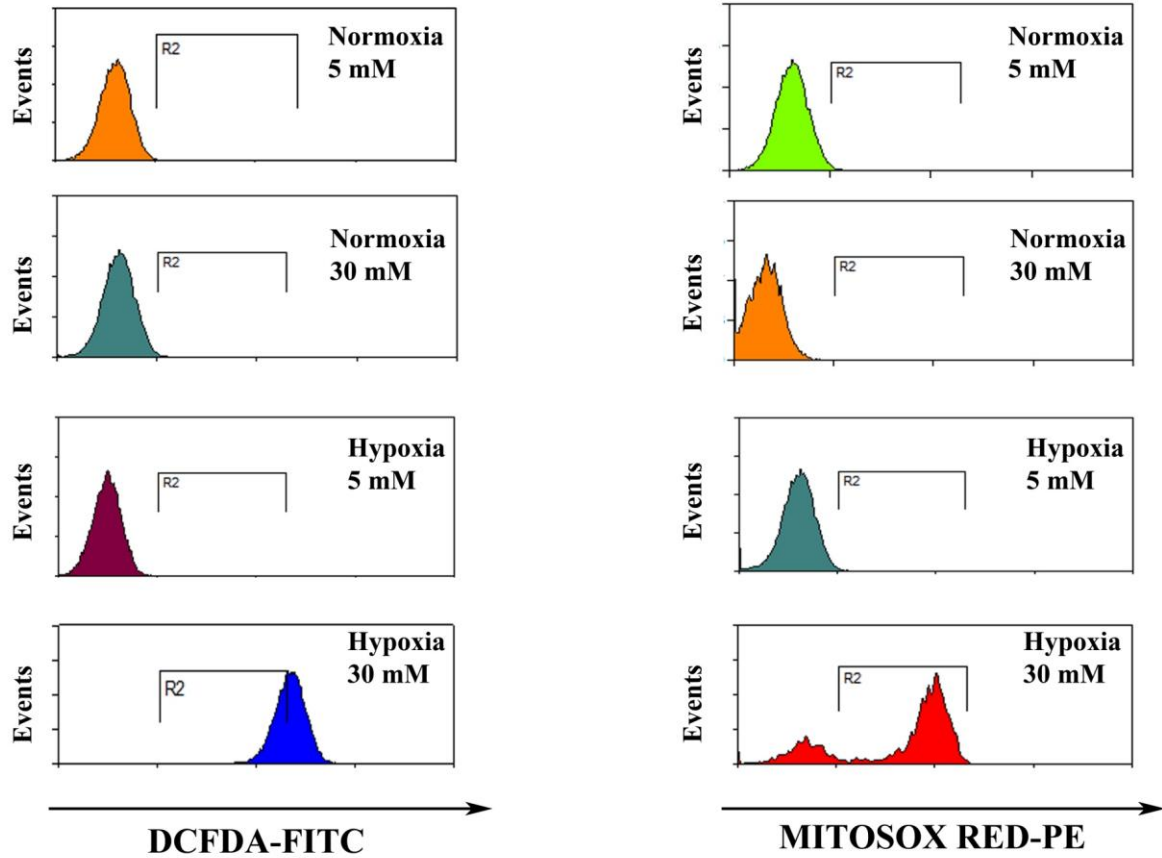
HDMEC CELL LINE

Figure 16. ROS detection in HDFs (upper panel) and HDMEC (lower panel) cells. The CM-H2DCFDA passively diffuses into cells, where its acetate groups are cleaved by intracellular. Subsequent oxidation yields a fluorescent adduct that is trapped inside the cell. The Mitosox Red targets superoxide in mitochondria.

High glucose and hypoxia trigger apoptosis

Our observation that the combination of hypoxia and hyperglycemia increased ROS production, prompted us to investigate the effect of ROS on apoptosis. We evaluated apoptosis by staining with Annexin V-FITC after a prolonged exposure of 5 days to hypoxia and hyperglycemia. As shown in figure 17, apoptotic cells were not detected neither in normoxia (either in low glucose or

high glucose,) nor in hypoxia and 5.5 mM glucose. The combination of hypoxia and hyperglycemia induces apoptosis, as shown by the percentage of cells Annexin V-FITC positive in Q4 quadrant. There is also an increase of cells in late apoptosis, as shown by the increase of Annexin V and PI staining in the Q2 quadrant. We hypothesized that the ROS overproduction enhanced by high glucose and hypoxia, accumulates damages in the cells and triggers apoptosis, which is detectable after a prolonged exposure to low oxygen levels and high glucose.
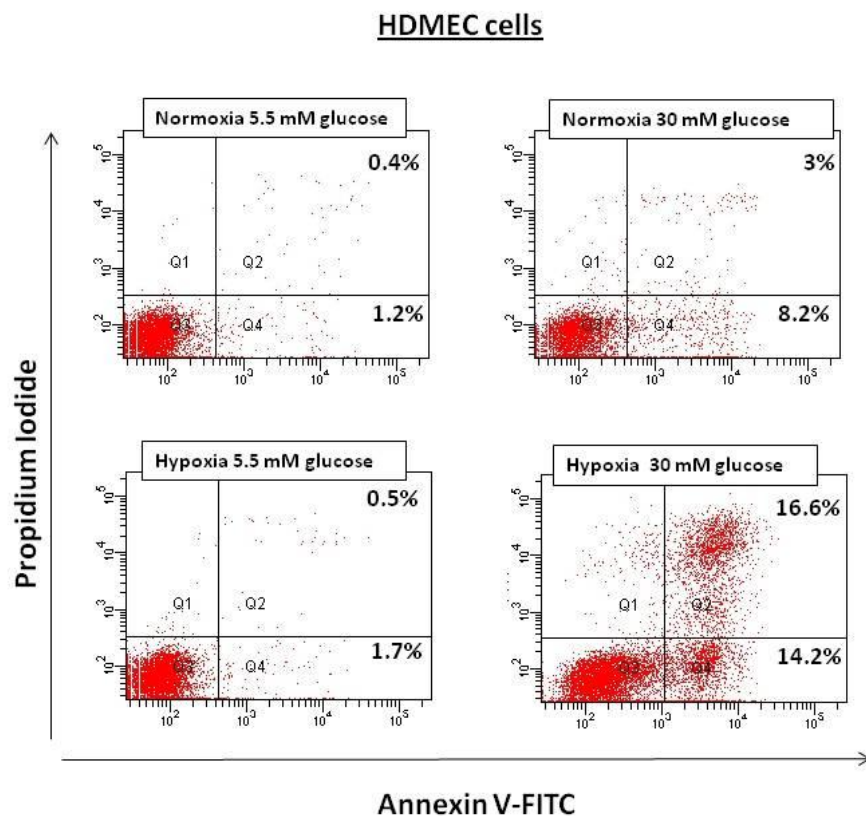

Figure 17. Flow cytometry analysis of apoptosis in HDMEC cells exposed to hyperglycemia and hypoxia and hyperglycemia. Representative of two separate experiments. Q1 shows necrotic cells PI positive; Q2, Annexin V and PI positive; Q3, live cells Annexin V and PI negative; Q4, apoptotic cells Annexin V positive.

Mitochondrial mass and mtDNA content in hyperglycemia in normoxia and hypoxia

In order to investigate the effect of high glucose on mitochondrial mass, we evaluated the mitochondrial content by measuring the activity of citrate synthase enzyme in HDFs and HDMEC after treatment with low glucose, high glucose and mannitol in hypoxia and normoxia for 3 and 5 days. The enzyme activity in normal growth condition (5.5 mM glucose in normoxia) was also evaluated and correspond to the activity at time 0.

In HDFs (figure 18a) in hypoxia, citrate synthase activity is reduced of about 35% ($P < 0.05$) after 3 days and the reduction is of 45% ($P < 0.05$) after 5 days, with respect to the control cells cultured in 5.5 mM glucose.

In HDMEC (figure 18b) in hypoxia, citrate synthase activity is reduced of about 27% ($P < 0.05$) after 3 days and the reduction is of 43% ($P < 0.05$) after 5 days. Each condition has been compared to the control cells, cultured in 5.5 mM glucose.

In both cell lines, the decrease in mitochondrial mass in hypoxia is independent of glucose concentration and mannitol. No significant differences in mitochondrial content have been observed in different experimental conditions in normoxia.
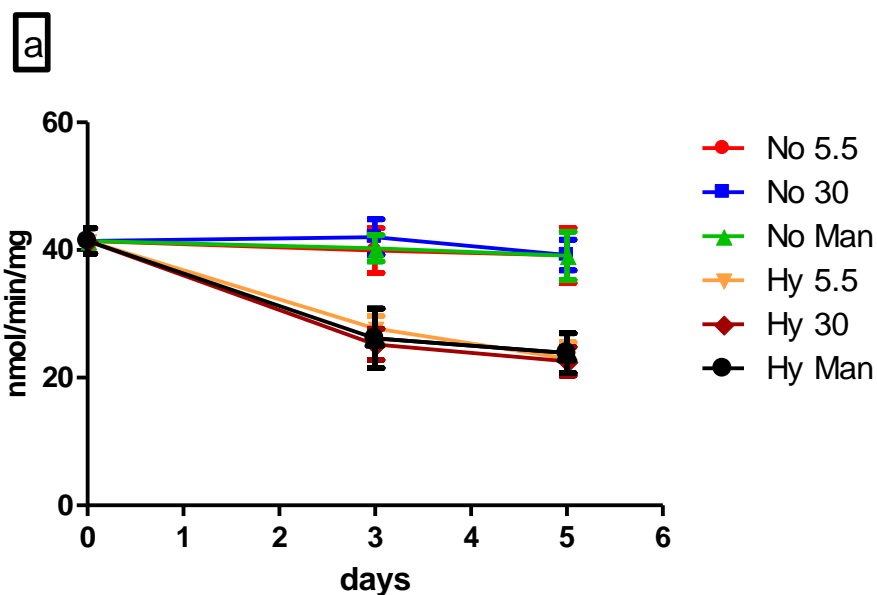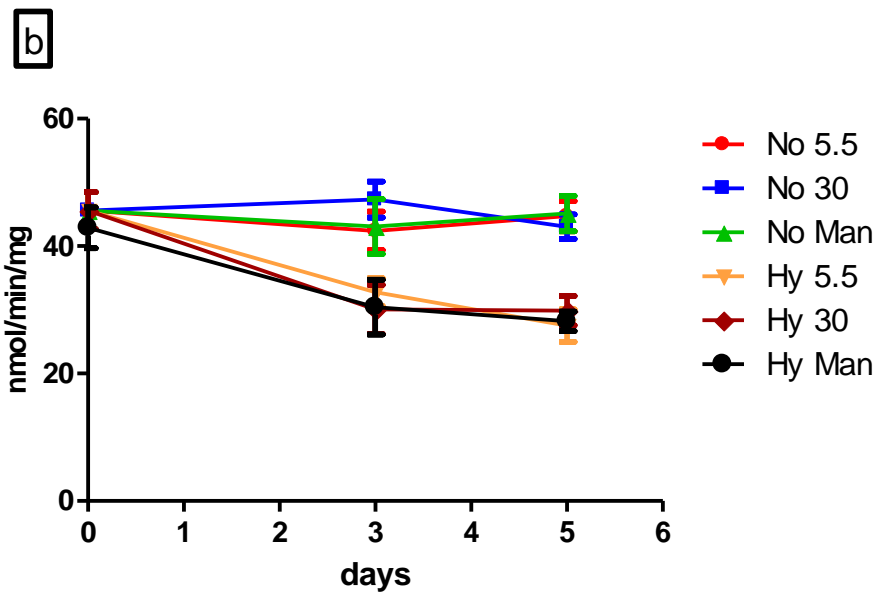
figure 18. Citrate Synthase activity in **a)** HDFs and **b)** HDMEC after 3 and 5 days in different experimental conditions.

It has been reported that under pathological conditions, mitochondrial abundance as well as the copy number of mtDNA in cells changes in response to increases in oxidative status. Since oxidative stress is elevated in the hyperglycemic state, we evaluated and compared the effect of only hyperglycemia in normoxia and combined hyperglycemia and hypoxia on mtDNA copy number.

In figure 19 and 20 the mtDNA content is shown in HDFs and HDMEC, respectively, after 5 days of exposure to hyperglycemia and both hyperglycemia and hypoxia. mtDNA copy number were evaluated by qPCR, measuring the ratio between mitochondrial gene cyt b and 16s rRNA and nuclear gene GAPDH. Despite hypoxia and/or hyperglycemia increase the oxidative stress, the analysis of both mitochondrial genes shows differences in mtDNA copy number only between normoxia and hypoxia, independently of glucose concentrations, suggesting that the reduction of mtDNA copy number is related to the decrease of the number of mitochondria in hypoxia.
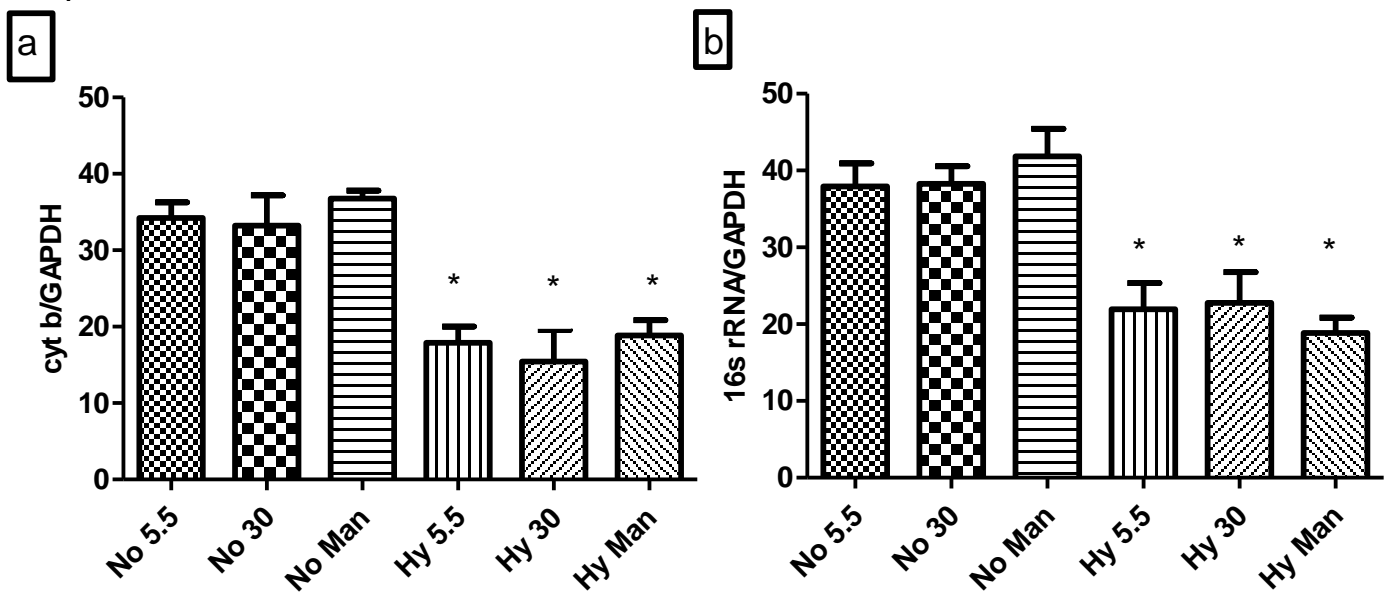
figure 19 Mitochondrial DNA copy number in HDFs. mtDNA copy number in fibrobasts was evaluated after the exposure to hyperglycemia (normoxia **No** and hypoxia **Hy**) and hyperglycemia plus hypoxia for 5 days. **a)** shows the ratio between mitochondrial cyt b and nuclear GAPDH **b)** shows the ratio between mitochondrial 16s rRNA and GAPDH. (P value <0.05, test di Dunnett vs 5mM glu in normoxia)

figure 20 Mitochondrial DNA copy number in HDMEC. mtDNA copy number in endothelial cells was evaluated after the exposure to hyperglycemia (normoxia **No** and hypoxia **Hy**) and hyperglycemia plus hypoxia for 5 days. **a)** shows the ratio between mitochondrial cyt b and nuclear GAPDH **b)** shows the ratio between mitochondrial 16s rRNA and GAPDH. (P value <0.05, test di Dunnett vs 5mM glu in normoxia)
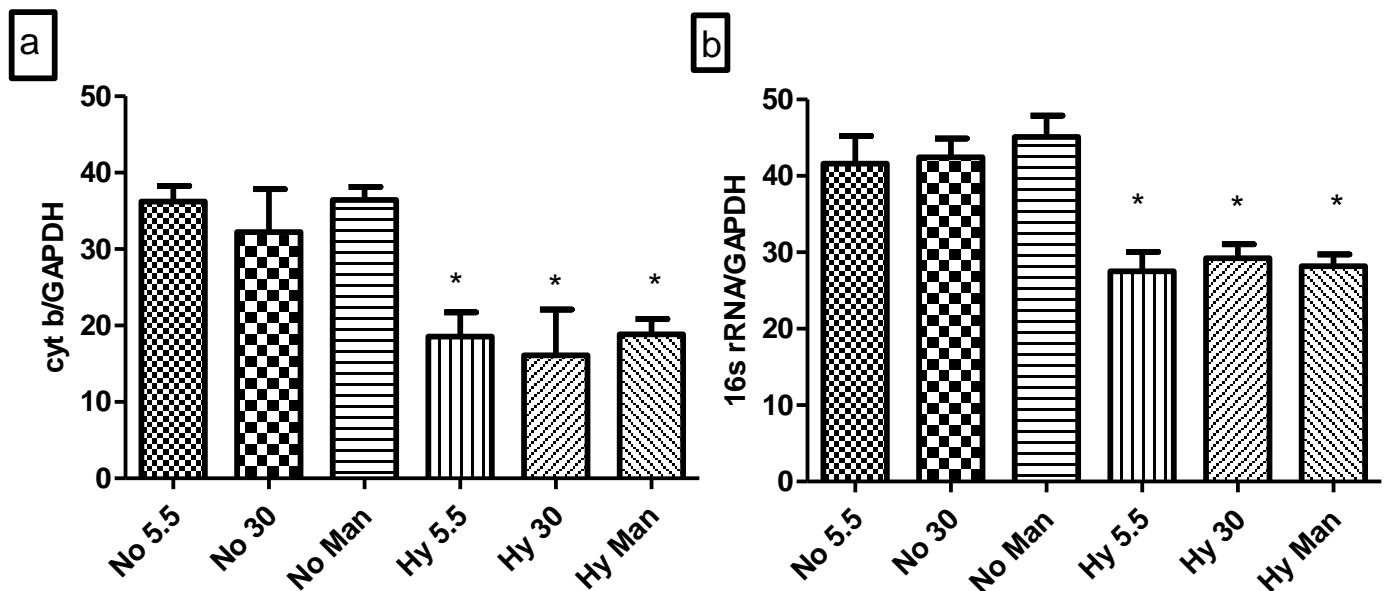
Discussion

Increasing evidence of experimental and clinical studies suggest that ROS play an important role in the pathogenesis of diabetes. Thus, ROS and in particular the overproduction of reactive oxygen species by the mitochondrial electron-transport chain, have been implicated in diabetic complications. In cells with high glucose inside, there is more glucose being oxidized in the TCA cycle, which in effect pushes more electron donors (NADH and FADH2) into the electron transport chain. As a result of this, the voltage gradient across the mitochondrial membrane increases until a critical threshold is reached. At this point, electron transfer inside complex III is blocked, causing the electrons to back up to coenzyme Q, which donates the electrons one at a time to molecular oxygen, thereby generating superoxide.

Several studies showed that hyperglycemia induces mitochondrial ROS production in rat mesengial cells [88]. Superoxide production was found increased also in leucocytes from patients with diabetes and retinopathy [89], in renal proximal tubular cells [90] and in rat isolated islets [91] and in bovine aortic endothelial cells [85]**.**

Hypoxia directly or through induction of ROS have been suggested to have an important role in the development of diabetic complication. The adaptative responses of the cells to hypoxia are mediated by HIF-1α and in 2008 Botusan IR [68], demonstrated that several HIF-regulated genes essential for different mechanisms activated in wound healing (i.e., migration, recruitment of CAG, and angiogenesis) were repressed in diabetic wounds.

Results presented in this dissertation show that, contrary to what have been reported, hyperglycemia does not induce ROS overproduction neither in HDFs nor in HDMEC cells cultured in high glucose for 18 hours, in normoxia . This might be explained by an adaptation of cells to hyperglycemia or a time-dependent effect of high glucose in generate reactive oxygen species, which might occur after several days when cells are cultured in normoxia. Indeed, the combination of both hypoxia and hyperglycemia increase ROS production either in HDFs or HDMEC. Based on a previous study where Kim et al. [42],

highlighted that hypoxia induced pyruvate dehydrogenase kinase 1 (PDK1) is critical for the attenuation of mitochondrial ROS production and adaptation to hypoxia and since hyperglycemia destabilizes HIF-1α [66], we hypothesized that HIF-1α destabilization increases the flux to oxidative phosphorylation through the inhibition of hypoxia-induced PDK1.

ROS measurement with DCFDA demonstrated that hypoxia and hyperglycemia cause ROS overproduction and Mitosox Red, a specific probe for mitochondrial reactive oxygen species, showed that the same treatment induces ROS overproduction from mitochondria.

It is well established that increased ROS production trigger apoptosis. Preliminary results on HDMEC, demonstrated that cells undergo apoptosis only after a prolonged (5 days) exposure to hypoxia and hyperglycemia, indicating that apoptosis in complications of diabetes might be a time-dependent process and that can be exacerbated when cells are exposed to hypoxia and high glucose for a longer period.

We also evaluated whether the prolonged exposure to hypoxia and hyperglycemia could modulate the mtDNA content and despite has been reported that hyperglycemia and increased ROS production can change it, we did not find any significant difference in normorxia and apparently, the reduction we found in hypoxia and high glucose reflects the decrease of mitochondrial mass as consequence of the lack of oxygen, as confirmed also by the lower citrate synthase activity in hypoxia. Since HIF-1α is induces BNIP3, a gene involved in autophagy of mitochondria, we expected to find a difference in mitochondrial content in cells exposed to hypoxia and high glucose and perhaps an increase, but our data showed that the mitochondrial content assayed by citrate synthase activity is not affected. Several studies reported that autophagy is also induced by Akt , JNK and FOXO transcription factor [92] or by mitochondrial ROS [93]. We hypothesized that , in cells cultured in hypoxia and hyperglycemia a balance between the loss of activation of autophagy by HIF-1α and the activation of the autophagy by ROS and FOXO transcription factor might establish. This also could be a pathogenic

mechanism that allows the accumulation of defective mitochondria and could be important for diabetes complications.

In conclusion, we show here that the exposure of HDFs and HDMEC cells to high glucose for 18 hours does not induce any change in ROS production, indeed the combination of low oxygen tension and high glucose induces ROS overproduction from mitochondria. We speculated that the increased ROS levels are dependent on HIF-1α destabilization and on the loss of the activation of PDK1 transcription, that is critical for the attenuation of ROS production and adaptation to hypoxia. Our data also showed that high glucose alone does not affect mtDNA content and mitochondrial mass and that in hypoxia and high glucose the decrease of both those parameters do not show significant differences with respect to low glucose in hypoxia. Further investigations in vitro will carried on a HIF-1α knocked out cell line to confirm the dependence of ROS overproduction in hypoxia and high glucose on HIF-1α destabilization, and afterwards we want to evaluate whether by reintroducing HIF-1α expression, it can rescue ROS overproduction. It might contribute to understand the pathogenic mechanisms involved in complications of diabetes to find new therapeutic targets.

3   MODULATION OF ATPase INHIBIYTORY FACTOR (IF1) EXPRESSION

Aim

Central to mitochondrial function is an electrochemical proton gradient across the mitochondrial inner membrane, that is established by the proton pumping activity of the respiratory chain. Impaired mitochondrial function, resulting from a variety of different mechanisms, will usually cause a decrease in $\Delta\psi_m$ as a common endpoint.

The ability of the F1F0-ATP synthase to reverse and act as an ATPase during conditions of reduced membrane potential has been appreciated for many years. ATP consumption by the F1Fo -ATPase could represent an important pathogenic mechanism in diseases in which mitochondrial respiration is compromised.

These diseases include the lack of oxygen or substrate (as in a stroke or heart attack), but also include many diseases in which more subtle defects in mitochondria are implicated, including Alzheimer's and motor neuron diseases and a large number of rare but debilitating diseases that involve genetic defects affecting mitochondrial proteins

The mammalian mitochondrial ATP synthase, consists of 15 different subunits, but a 16th subunit is also present, the IF1 inhibitor, a protein which binds at the α/β catalytic sites and inhibits ATP hydrolysis. The binding of IF1 to F1 is pH dependent being optimal at pH around neutrality [23].

When the aerobic proton motive force declines, like in ischemia or respiratory substrate deficiency, decrease of the matrix pH promotes binding of IF1 to F1, with prevention of ATP hydrolysis.

In conditions of normal generation of the respiratory electrochemical proton gradient, resulting in pH increase in the matrix space, IF1 dissociates from the catalytic sites and ATP synthesis takes place normally.

The expression of IF1 in human tissues and its participation in the development of human pathology are unknown.

Recently, Campanella et al. [21], found that IF1 is important in regulating the mitochondrial fraction. When IF1 was overexpressed the fraction of the cell volume occupied by mitochondria was significantly increased compared to controls with basal IF1 expression levels. Conversely, suppression of IF1 promoted the opposite result with a decrease in mitochondrial fraction. Thus, overexpression of IF1 also has a role in remodeling mitochondrial cristae and might have a role as "coupling factor" increasing the efficiency of oxidative phosphorylation.

On the opposite, Sanchez-Cenizo L. et al. [94], demonstrated that IF1 plays a role in limiting oxidative phosphorylation and thus in promoting glycolysis.

Taken together these results, the aim of this study was to characterize the bioenergetics of cell lines with different expression levels of IF1, modulated by silencing and overexpression, in particular when cells are grown in hypoxia, a condition that can mimic different pathologies, such as cancer or heart disease.

Plasmid construct

IF1 cDNA was transferred from the original pCMV6-XL4 plasmid, which allows transient transfection in mammalian cells, into the pCDNA3 plasmid, that allows to perform stable transfection and select stable cell clones over-expressing IF1 by the selection with the antibiotic G418. In figure 21 the plasmids used for cloning are shown, both of them contain a *polylinker region,* where enzyme restriction sites are present, SV40 ori that allows for replication in mammalian cells and f1 Ori, the philamentous phage origin of replication, which allows for the recovery of single-stranded plasmids. Selection of the plasmid in E.coli is conferred by the ampicillin resistance gene. Only pCDNA3 has the gene for the resistance to Neomycin/G418 used for selecting eucariotic cell clones. To cloning IF1 cDNA in pcDNA3 plasmid , a

570 bp IF1 fragment was digested with NotI restriction enzyme from pCMV6-XL4-IF1 plasmid, and inserted in-frame into the pCDNA3 plasmid digested and linearized with the same enzyme NotI.
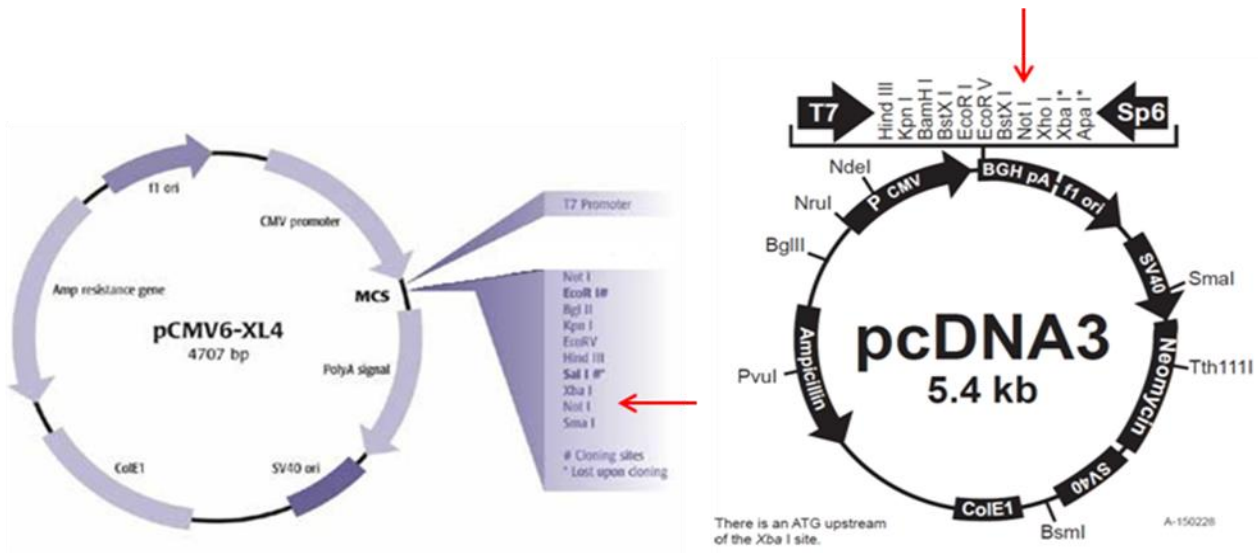

Figure 21. Representation of the plasmidic vector used for cloning. Red arrows show the restriction sites of Not I enzyme into the polylinker region.

After ligation reaction by T4 DNA Ligase, which join two strands of DNA between the 5'-phosphate and the 3'-hydroxyl groups of adjacent nucleotides in either sticky- or blunt-end configuration, the insertion and the correct orientation of IF1 cDNA have been checked by PCR. Fig 22a is a schematic representation of the primers binding sites and the 375 bp amplification product obtained by amplification. Figure 22b shows the amplification products obtained by PCR analysis with the same primers on 24 bacterial colonies.

The black arrows indicate the 375 bp fragment obtained by amplification in four bacterial colonies.
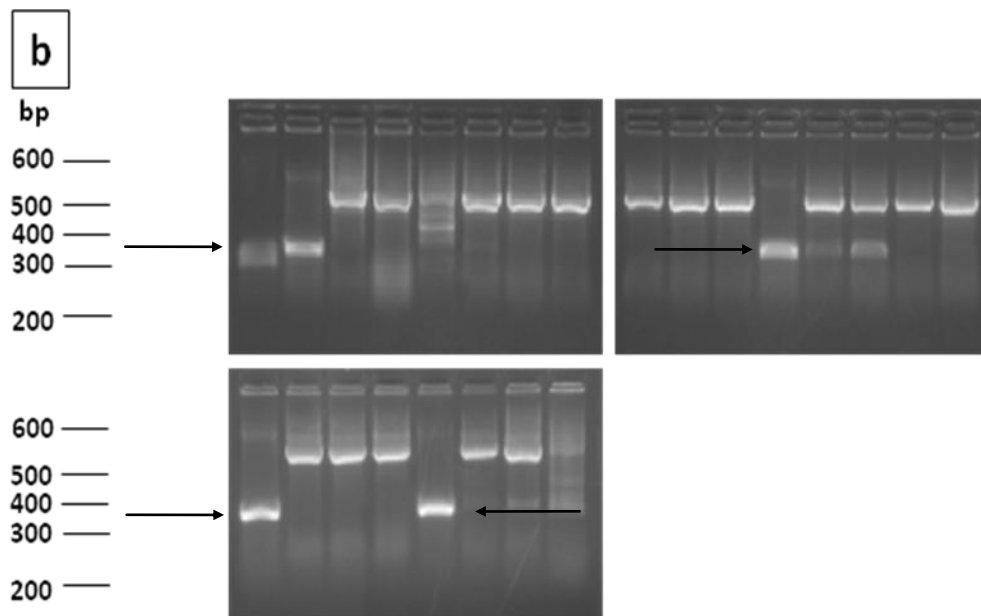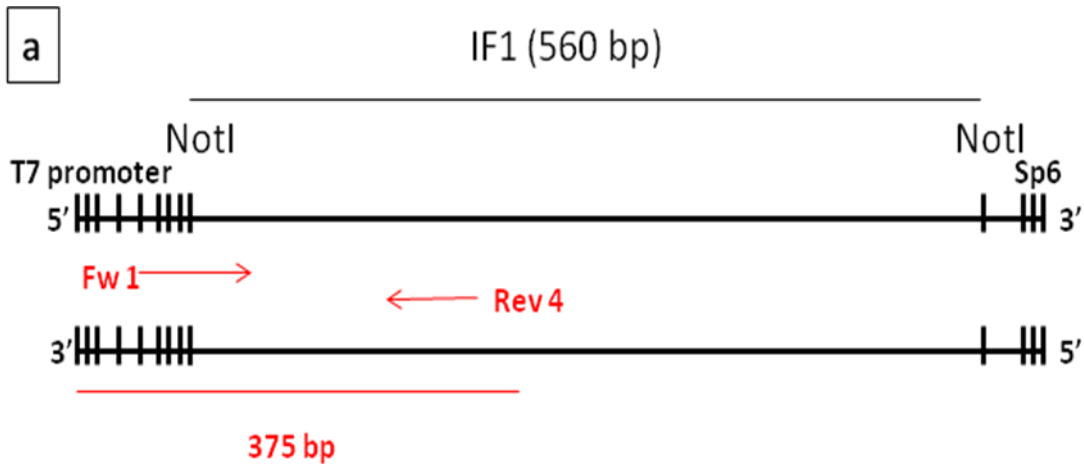
figure 22. **a)** The figure shows the site where the primers bind. The forward 1 binds to the T7 promoter region and the reverse 4 binds to the internal region of IF1 gene sequence. **b)** 1,2% agarose (EtBr 500 µg/ml) gel used for the screening of IF1 insertion into 24 bacterial colonies.

To verify IF1 insert into the four plasmid was not mutated, analysis by sequencing was carried out. The four plasmids have been sequenced using the forward primer that binds to the T7 promoter on the filament 5'-3' and the reverse primer that binds to the BGH promoter on the filament 3'-5'. Figure 23

shows the representative alignement of the sequence of one bacterial plasmid, analyzed by sequencing. The perfect alignement between IF1 sequences analyzed by sequencing and the registered IF1 sequence shows that IF1 gene have not been affected by any point mutation during the cloning process. After cell transfection, several stable cell clone have been selected by the antibiotic G418 and IF1 expression has been analyzed by Western Blot. Figure 24 shows IF1 expression in one pcDNA3-IF1 transfected cell clone compared with the control line of 143B transfected with empty pcDNA3. The quantification analysis indicates that IF1 expression is 2,5 times more in pcDNA3-IF1 than in pcDNA3 scramble; the overexpression was quantified (data not shown) and has been normalized versus the ATP synthase D subunit content.
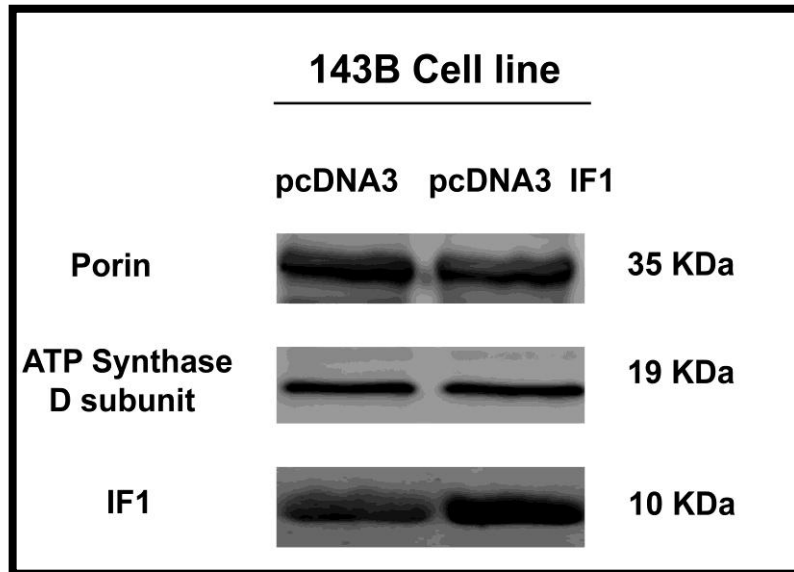
Fig. 23 Alignment of IF1 sequence inserted into the pcDNA3 with the registered IF1 sequence on NIH database. Red squares indicate Not I sites, used for cloning IF1 in pcDNA3. Sequences have been analyzed by BMR Genomics s.r.l, Padova, Italy

figure 24 Western Blot analysis of IF1 expression in 143B cells transfected with pcDNA3 empty (left) and pcDNA3-IF1 (right)

Effect of IF1 over-expression on ATP hydrolysis and membrane potential

The effect of IF1 over-expression has been investigating measuring ATP hydrolysis activity in mitochondria isolated from the parental 143B cell line transfected with the empty vector and from the stable cell line over-expressing IF1 gene. Since IF1 binds ATP synthase when pH in the matrix drops to about 6.7, isolated mitochondria have been resuspended in Hepes-buffer with two different pH, one at 6.7 to promote IF1 binding to ATP synthase and the other at 7.4 in order to find the best experimental conditions for the assay . In figure 25 the ATPase hydrolysis activity is shown in two different pH conditions and it is expressed as nmol per mg of cellular protein per minute (nmol/min/mg). ATP hydrolysis activity in 143B control cells is reduced of 45% when IF1 binding to ATP synthase is stimulated by the pH; the reduction of the activity at pH 6.7 in

the clone over-expressing IF1 is greater (-57%) with respect to the condition at pH 7.4. Moreover, in the stable clone even when the pH does not allow the binding of IF1 to ATP synthase, we observed a modest reduction of ATP hydrolysis

(-25%) as compared with parental143B cell line at pH 7.4. Our results show that the cells overexpressing IF1 have a reduced ATP hydrolysis activity, as consequence of the increased expression levels of IF1.
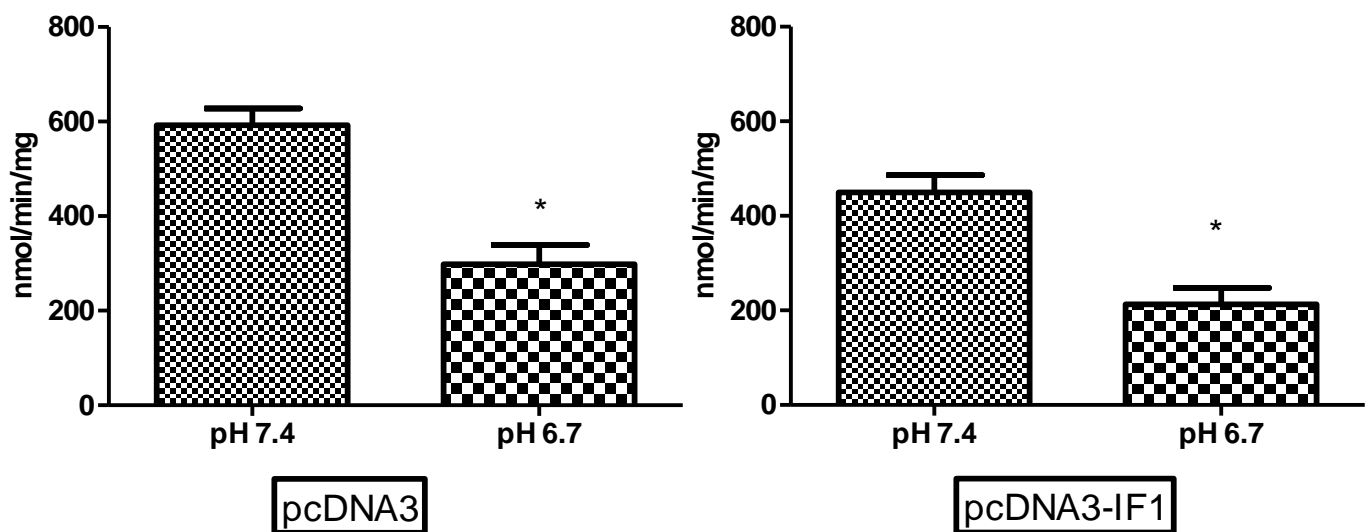

figure 25 ATP hydrolysis in 143 B cells transfected with scramble pcDNA3 (left) and pcDNA3-IF1 (right). (* P<0.05, statistical analysis was performed with Student t test)

We also evaluated the effect of IF1 overexpression on mitochondrial membrane potential. We measured the membrane potential by the fluorescent probe TetraMethylRhodamine Methyl estere (TMRM), a cell-permeant, cationic, red-orange fluorescent dye that is readily sequestered by active mitochondria. Fluorescent images in figure 26 show the membrane potential in normal growth conditions, that is comparable in both cell lines. When Antimycin A, Complex III inhibitor was added, we observed a decrease of TMRM fluorescence, as consequence of the block of proton translocation and a reduction of the membrane potential. In 143B cells overexpressing IF1, the decrease of the fluorescence is greater as shown by the quantification (figure 26, lower panel). This decrease confirms that the clone overexpressing IF1 is

not able to maintain the membrane potential by the hydrolysis of ATP, as reported by ATP hydrolysis assay , since IF1 protein binds ATP synthase.. When oligomycin, a Complex V inhibitor, is added membrane potential drops in both cell lines, as consequence of the block of proton translocation and membrane depolarization .
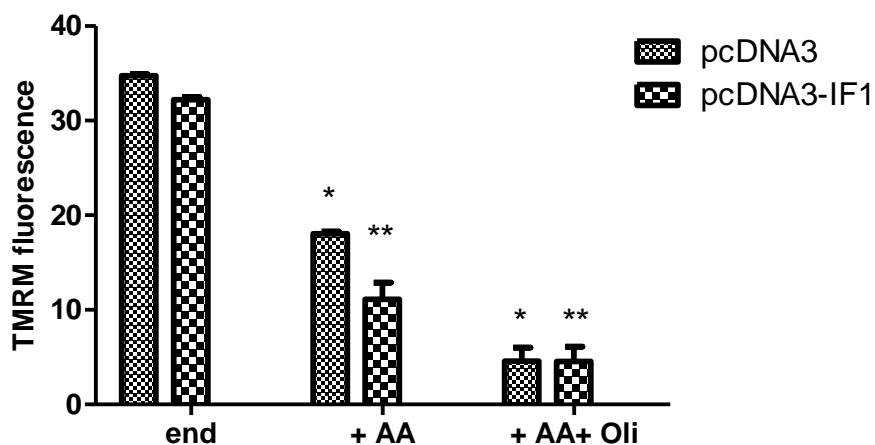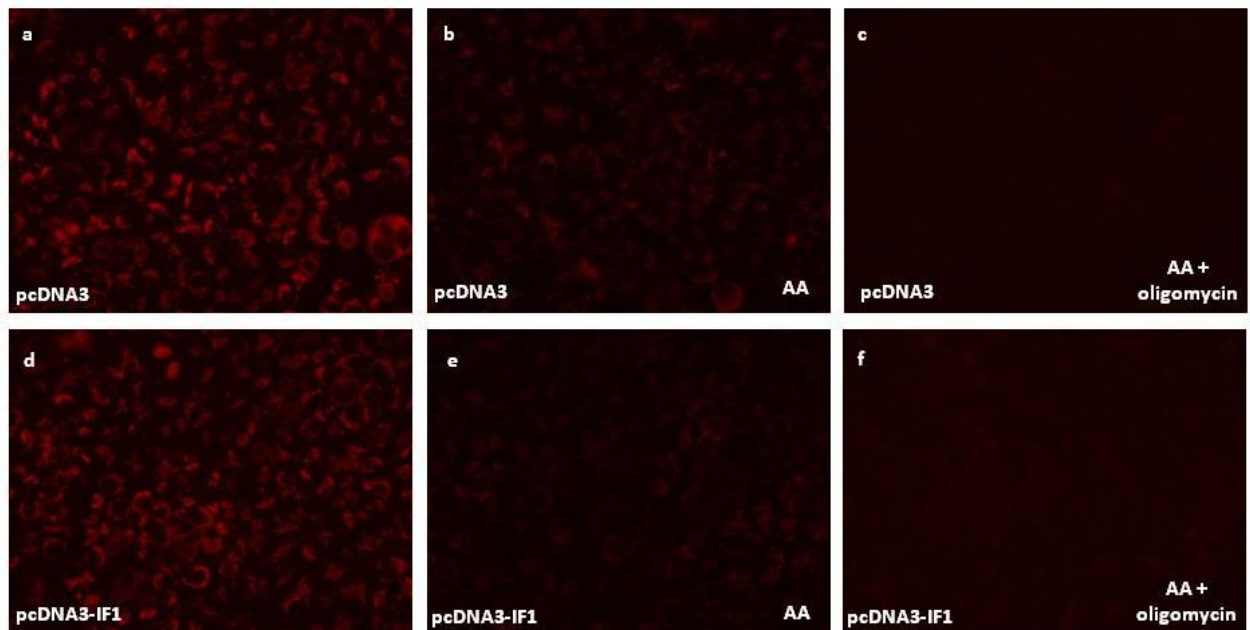
Figure 26 . Mitochondrial membran potential measured by fluorescent microscopy using the probeTMRM . In a) and d) is shown the endogenous membran potential; in b) and e) cells have been incubated with Antimycin A (AA); in c) and f) cells have been incubated with AA and oligomycin.In the lower panel TMRM fluorescence was quantified using the software ImageJ (*p value<0.05 respect to pcDNA3 end; **p valu<0.05 respect to pcDNA3-IF1 end).

Discussion

The aim of this project was to study how cells reply to a modulation of IF1 expression, when they are cultured in physiological oxygen levels (21%) or in low oxygen conditions, mild hypoxia (1%) or severe hypoxia (0.5%).

Most of the work for this study has been carried out in cloning the IF1 cDNA into a plasmid suitable for a stable transfection and for checking that the IF1 insertion into the plasmid did not affect the cDNA and promoters sequences with any point mutation.

In this thesis, we showed few preliminary results obtaneid comparing the parental 143B cell line and the clone overexpressing IF1, cultured at physiological oxygen levels (21%).

The first evidence, as shown by western blot analysis, is that in stable clone IF1 expression level is more than 2 times higher than in the parental cell line.

The ATP hydrolysis assay indicated that cells overexpressing IF1 have defective ATP hydrolysis ability when IF1 binding to ATP synthase is stimulated. This has been confirmed also by measuring the membrane potential in presence of antimycin A, that is lower in the clone overexpressing IF1, indicating that when the $\Delta\psi_m$ drops IF1 binds to ATP synthase and inhibits ATP hydrolysis, that is activated to mantaine the membrane potential.

These data indicated that the cloning process has been seen out and that IF1 is able to perform its physiological role in inhibiting ATP hydrolysis when the binding to ATP synthase is stimulated, for istance by the pH.

Since the effect of IF1 on ATP synthesis is still unclear, this project will be carried on in our lab and 143B control cell line and the clone overexpressing IF1 will be compared in normoxia and hypoxia, to evaluate how the modulation of IF1 expression levels can affect the bioenergetics of these cells; ATP synthesis rate will be evaluated in addition to ATP hydrolysis. Moreover, exposure of the cells to hypoxia can mimic the condition of stroke, where ATP consumption by the ATPase activity could represent an important pathogenic mechanism and it will be interesting to evaluate whether the overexpression of

IF1 is protective to cells and reduces cell death in response to oxygen deprivation, as observed in vivo on rat heart [95].

Materials and Methods

Cell Culture

Fibroblasts were obtained from skin biopsies and cell lines were established in Dulbecco's modified Eagle's medium (DMEM) containing 25 mM glucose supplemented with 15 % fetal bovine serum (FBS). During the study fibroblasts were cultured in DMEM containing 5 mM glucose, 100 U/ml penicillin, 100 µg/ml streptomycin, 0.25 µg/ml amphotericin B, 4 mM glutamine and 1 mM pyruvate.

Fibroblasts were seeded the day before the experiments to favour adhesion, and after 12 hours the medium was replaced with fresh media and cells were cultured in two different incubators at 37°C in a humidified atmosphere of 5% CO_2 under normal (21%) and low (0.5-4%) oxygen tension. Low O_2 concentrations were obtained using the $INVIVO_{200}$ hypoxia workstation (Ruskinn Technology Ltd, UK) equipped with the gas mixer Q to obtain accurate control and stability of O_2 and CO_2 concentrations.

HDFs, HDMECs and culture media were purchased from PromoCell (Heidelberg, Germany). All other cell culture reagents were from Gibco (Stockholm, Sweden). D-Glucose and Mannitol were purchased from Sigma (St. Louis, MO). Cell lines were maintained in a humidified atmosphere with 5% CO2 at 37°C in commercially supplied fibroblast and endothelial cell growth media.

HDF and HDMECs were established in Dulbecco's modified Eagle's medium (DMEM) containing 5.5 mM glucose supplemented with 2 mM L-glutamine, 100 IU/ml penicillin and streptomycin and 10 % fetal bovine serum (FBS) and cells between passages 4 and 9 were used.

During the experiments cell lines were cultured in DMEM containing 5.5 mM glucose and 30 mM glucose in two different incubators at 37°C in a humidified atmosphere of 5% CO_2 under normal (21%) and low (0,5-1%) oxygen tension. Low oxygen concentrations were obtained using the $INVIVO_{200}$ hypoxia chamber (Ruskin Technology Ltd, UK).

Osteosarcoma cell line 143B was cultured in Dulbecco's modified Eagle's medium (DMEM) containing 25 mM glucose, 1 mM pyruvate and 4 mM

glutamine (Sigma-Aldrich) supplemented with 10 % fetal bovine serum (FBS). The medium used for cell culture contained also 100 U/ml penicillin, 100 µg/ml streptomycin, 0.25 µg/ml amphotericin B. FBS, penicillin, streptomycin and amphotericin B were purchased from Gibco.

Cell Growth Evaluation

Cell growth was assayed after culturing fibroblasts in different oxygen levels (from 21% to 0.5%) for 72 hours. Cells were washed with phosphate-buffered saline (PBS), trypsinized, collected, and the fibroblasts viability was assessed using trypan blue.

Mitochondrial ATP Synthesis Assay and Cellular ATP Content

The oligomycin-sensitive ATP synthase activity in permeabilized fibroblasts was determined according to the method described by Sgarbi et al., 2006. Essentially, fibroblasts (2×10^6 cells/ml) were incubated for 15 min with 60 µg/ml digitonin in a Tris/Cl buffer (pH 7.4). Complex I driven ATP synthesis was induced by adding 10 mM glutamate/malate (+ 0.6 mM malonate) and 0.5 mM ADP to the sample. The reaction was stopped 3 min later by adding dimethylsulphoxide, and both newly synthesised ATP and intracellular ATP were measured by bioluminescence using a luciferin–luciferase system (ATP bioluminescent assay kit CLS II; Roche, Basel, Switzerland) according to the manufacturer's instructions. The amount of ATP measured was referred to the protein content, determined by the method of Lowry. The rate of ATP synthesis was expressed as nmol/min/mg protein and the intracellular ATP content as nmol/mg protein.

Citrate Synthase Assay

The citrate synthase activity was assayed essentially as described in Trounce et al. 1996 [96] by incubating samples in 125 mM Tris pH 8 with 0.2% Triton X-100, and monitoring the reaction at 30°C by measuring spectrophotometrically the rate of free coenzyme A (90 μM) release at 412 nm. The citrate synthase activity has been considered as a general marker for mitochondrial volume in cells and its value was utilized for normalization of other mitochondrial activities.

Analysis of Intracellular ROS in Live Cells

Fibroblasts grown on multiwells plates for 72 hours at 21% and 1% O_2, were washed once with PBS and loaded with 5 μM 2′,7′-dichlorofluorescin diacetate (DCF-DA, Molecular Probes) in complete medium without FBS for 30 minutes in the dark. After loading, the dye was removed by washing the cells twice with PBS, and intracellular ROS content was detected by measuring the fluorescence emission at 535 nm in a Wallac Victor2 1420 multilabel counter (Perkin-Elmer), according to Baracca [97].

Electrophoresis and Western Blot Analysis in Cell Lysates

Fibroblasts grown for 72 hours under 21% and 1% O_2 were lysed in 50 mM Tris, pH 8.0, 150 mM NaCl, 1% SDS, 1% Triton X-100, 0.55% DOC, 1 mM PMSF, and 100 μg/ml of protease inhibitors. The protein content was determined by Lowry method and equal amounts of cell lysate was separated by SDS-PAGE and blotted onto nitrocellulose membrane.

The membranes were saturated overnight in blocking solution (KH2PO4 1 mM, NaCl 150 mM, NaH2PO4 3 mM pH 7,4 containing 0.05% Tween-20, 2% non-fat dry milk and 2% bovine serum albumin). Non-bound antibodies were removed by washing in PBS-0.05% Tween-20 solution. Membranes were incubated with five primary mouse monoclonal antibodies specific for single subunits of each OXPHOS complex as follows: NDUFA9 (39 kDa) of Complex I, SDHA (70 kDa) of Complex II, Rieske protein (22 kDa, apparent molecular weight is 30 kDa) of Complex III, COX-I (57 kDa, apparent 45 kDa) of Complex IV, subunit β of F_1F_0-ATPase (52 kDa) (MitoSciences Inc., Eugene, OR, USA). To correct the amount of each protein complex to the cellular mitochondrial content, porin (31 kDa) was immunodetected with mouse anti-porin primary antibody (Molecular Probes).

Intracellular ROS measurement by flow citometry

HDF and HDMEC were seeded in multiwells plates in 5.5 mM glucose and after 18 hours the media was replaced starting the treatments in hyperglycemia (30 mM glucose) and hypoxia (1% oxygen tension). After 5 days, cells were washed once with Phosphate Buffered Saline (PBS) and loaded with 5 µM Mitososx Red (Molecular Probes) and carboxy methyl 2'-7' dichlorofluorescin diacetate (CMDCF-DA, Molecular Probes) in complete medium devoid of FBS for 3 hours minutes in the dark. After probe staining cells were harvested, washed twice with PBS and Mitosox Red and DCF fluorescence, index of intracellular ROS content, were detected by flow cytometry (Cyan, Beckman Coulter).

Annexin V-FITC/PI staining

To assess the extent of apoptosis induction after hypoxic and hyperglycemic treatments, flow cytometric analysis of Annexin V-FITC/PI-stained samples was performed.

HDMEC cells were seeded in multiwells plates at a density of 2500/cm^2 in complete medium containing 5,5 mM glucose. After 18 hours media were replaced and treatments in hyperglycemia and hypoxia (0,5%) started. After 5 days cells were detached, washed once in PBS and resuspended in Annexin V/PI (Bender MedSystem GmbH), according to manufacture instructions. Samples were analyzed by Cyan flow cytometer (Beckman Coulter, Miami, FL, USA) and at least 20.000 events per sample were acquired.

mtDNA copy number

To determine the amount of mtDNA present in each experimental condition, we used quantitative real-time PCR (qPCR) by measuring the ratio between the mitochondrial genes cyt b and 16S rRNA and the nuclear gene GAPDH. Total DNA was extracted from HDF and HDMEC cells cultured in different glucose concentrations and oxygen tensions. Total DNA was extracted by means of Qlamp DNA Blood Mini kit (QiAgen, Sweden) according to the manufacturer's instructions and the DNA concentration was measured by a NanoDrop ND-1000 spectrophotometer. To determine the ratio of 16S rRNA/GAPDH and cytb/GAPDH, qPCR was performed in an Applied Biosystems 7300 unit using Platinum SYBR Green quantitative PCR Supermix-UDG with ROX reference dye (Invitrogen). The primers used for cytb, 16s RNA and GAPDH amplification were synthesized by MWG Operon (Germany) and the sequences were as follows:

Cyt b   sense: 5'-ACATCGGCATTATCCTCCTG-3'

antisense: 5'-GTGTGAGGGTGGGACTGTCT-3'

16s rRNA   sense: 5′-ACTTTGCAAGGAGAGCCAAA-3′,

antisense: 5′-TGGACAACCAGCTATCACCA-3′.

GAPDH   sense: 5′-GGATGATGTTCTGGAAGAGCC-3′,

antisense: 5′-AACAGCCTCAAGATCATCAGC-3′.

PCR reactions were carried out under standard conditions, with 40 cycles using 5 ng of total DNA template in a 20 μL volume, containing SYBRGreen Supermix (including MgCl2, DNA polymerase, dNTP and SYBR) and 10 pmol of each primer. PCR cycles were performed as follow: 15 seconds of denaturation step at 95°C, and 15 seconds of hybridization and extension step at 60°C. The results are shown as $\Delta(\Delta Ct)$ values, $\Delta Ct = Ct_{cytb\ or\ 16s\ rRNA} - Ct_{GADPH}$, $\Delta\Delta Ct = \Delta Ct_{sample} - \Delta Ct_{CTRL}$.

Plasmid Construct

To generate an eukaryotic expression vector to allow for a stable cell line transfection we used the pCMV6-XL4 True Clone plasmid containing human ATPase-IF1 variant 1 cDNA (Origene) and the pcDNA3 plasmid with Neomycin resistance as selectable marker (Invitrogen).

Briefly, IF1 cDNA fragment was liberated from pCMV6-XL5 digesting the plasmid with Not I restriction enzyme for 4 hours at 37°C, according to the manufacture instructions, being present two Not I sites flanking the cloning site of the plasmid. IF1 insert has been separated from the plasmid by 1% agarose gel electophoresis and afterwards has been purified with the Wizard SV Gel and PCR Clean-up System (Promega). Concomitantly pCDNA3 plasmid has been linearized with Not I restriction enzyme (as described above) and then purified in 1,2 % agarose gel electrophoresis. Linear pCDNA3 was treated with tSAP enzyme (Promega) for 45 minutes at 37°C, to avoid the recircularization of the plasmid. To stop the tSAP treatment, the reaction mixture was heated at 75°C for 15 minutes. Finally tSAP treated linear pcDNA3 has been mixed with the IF1 fragment in a ligation reaction with T4 Ligase enzyme (Promega), for 3 hours at room temperature to obtain the circular pcDNA3-IF1.

Bacterial Transformation

Competent DH5α- E. Coli cells were transformed following standard protocol. Briefly, the ligation products were added to the bacteria, left in ice for 10 minutes, heated at 42°C for 45 seconds and cooled 2 minutes in ice. Than bacteria were grown for 1 hour in 1 ml of SOC medium, composed of 20 gr/L LB broth , 1M $MgCl_2$, 1M $MgSO_4$, 2M Glucose (Sigma-Aldrich). Bacterial colonies transformed with pCDNA3-IF1 plasmid were selected in 35 gr/L LB agar plates containing 100 µg/ml Ampicillin (Sigma-Aldrich).

Each colony was collected, expanded at 37°C overnight in 20 gr/L LB broth with 100 µg/ml Ampicillin and finally the plasmid DNA was purified from bacteria using Pure Yeld plasmid Miniprep kit (Promega), according to manufacture instructions.

Four purified plasmids were selected and IF1 corrected orientation was checked by PCR, using the following pairs of primers: T7 promoter forward primer 5'-TAA TAC GAC TCA CTA TAG GG-3' and the reverse internal primer R4 5'-AAA TAT CGT TCC TCT TCA GC-3'.

To check for the absence of point mutation in the IF1 cloned fragment we also sequenced each plasmid DNA using the T7 promoter forward primer and BGH reverse primer 5'-TAG AAG GCA CAG TCG AGG-3'.

Cell transfection

143 B cells were seeded the day before transfection in 35 mm plates. Seeding depends on cell lines growth and the transfection was performed when the confluence was about 40-60%.

The following day, the medium was replaced with 2 ml of DMEM (non so se è complete o devoid of FBS) (Sigma-Aldrich). 2µg of both pCDNA3-IF1 and pcDNA3 empty plasmids have been incubated, separately, with PEI-Polyethylenimine linear, MW ~25,000 (Polysciences, Inc) in DMEM for 20 minutes, using a 3:1 PEI:DNA ratio. The transfection mix was added to the

cells and 18-24h after transfection the medium was replaced with fresh medium containing 500 µg /ml of G418. to select clones over-expressing IF1 .After two weeks of selection, cell clones overexpressing IF1 were evaluated in by Western Blotting and the clone with the highest expression of IF1 were chosen to be expanded and used in the experiment

Mitochondrial Isolation

Two 143B clones, carrying the pCDNA3-IF1 and the empty pCDNA3 plasmids respectively, have been harvested and resuspended in extraction buffer pH 6.7 (0,07 M saccarose, 0,22 M manitol, 20 mM HEPES, 1 mM EDTA, 100 µM EGTA, 0.4% BSA). Cells have been mechanically disrupted using Potter-Elvehjem homogenizer and mitochondria were obtained by differential centrifugations and finally resuspended in two HEPES-buffer (20 mM HEPES, 2 mM MgCl2, 1 mM ATP) differenig by the pH: pH 6.7 was used to facilitate IF1 binding to ATPase and pH 7.4 to conversely maintein IF1 in the unbound form. Protein content was assessed spectrophotometrically (λ= 750 nm) by Lowry's method in presence of 0.3% (w/v) sodium deoxycholate. Bovine serum albumin was used as standard.

ATP hydrolysis Assay

ATPase activity was determined spectrophotometrically measuring the oxidation of NADH at 340 nm obtained coupling two reactions catalysed by pyruvate kinase (PK) and lactate dehydrogenase (LDH) respectively in presence of phosphoenolpyruvate (PEP).
The assay was performed in 25 mM TRIS/acetate pH 7.4, 25 mM KOH, 5 mM MgCl$_2$ and 30 µg of mitochondria were incubated with 4mM ATP, 160 µM NADH, 5 µM Rotenon, 1,5 mM PEP and LDH/PK. F1Fo ATPase activity has

been calculated as the difference between total and oligomicin-sensitive ATPase activity and finally was expressed as nmol/min/mg.

Mitochondrial membrane potential

Mitochondrial membrane potential in intact cells was evaluated by incubating cells over-expressing IF1 and cells carryng the empty vector with 20 nM Tetramethyl Rhodamine Methyl Ester (TMRM, Molecular Probes) for 30 minutes at 37°C in a humidified atmosphere of 5% CO_2 21% O_2. Cells were incubated in control conditions, in presence of 1 µg/ml antimycin A and in presence of antimycin A plus/together with 2 µM oligomycin. Images were acquired using a fluorescence inverted microscope (Olympus IX50). Antimycin A and oligomycin where purchased from Sigma-Aldrich. TMRM fluorescence intensity was evaluated by means of Image J software (http://rsbweb.nih.gov).

Statistic analysis

Differences of each experimental condition were evaluated by one-way ANOVA as appropriate, using Dunnett test and two-way ANOVA with Bonferroni post-hoc test. A p-value < 0.05 was considered statistically significant.

For ATP hydrolysis experiments, differences were evaluating by Student t test and p-values <0.05 were considered statistically significant.

References

1. Benard, G. and R. Rossignol, *Ultrastructure of the mitochondrion and its bearing on function and bioenergetics.* Antioxid Redox Signal, 2008. **10**(8): p. 1313-42.

2. Distler, A.M., et al., *Post-translational modifications of mitochondrial outer membrane proteins.* Methods Enzymol, 2009. **457**: p. 97-115.

3. Rimessi, A., et al., *The versatility of mitochondrial calcium signals: from stimulation of cell metabolism to induction of cell death.* Biochim Biophys Acta, 2008. **1777**(7-8): p. 808-16.

4. Frey, T.G. and C.A. Mannella, *The internal structure of mitochondria.* Trends Biochem Sci, 2000. **25**(7): p. 319-24.

5. Wallace, D.C., *A mitochondrial paradigm of metabolic and degenerative diseases, aging, and cancer: a dawn for evolutionary medicine.* Annu Rev Genet, 2005. **39**: p. 359-407.

6. Shoubridge, E.A. and T. Wai, *Mitochondrial DNA and the mammalian oocyte.* Curr Top Dev Biol, 2007. **77**: p. 87-111.

7. Chen, X.J. and R.A. Butow, *The organization and inheritance of the mitochondrial genome.* Nat Rev Genet, 2005. **6**(11): p. 815-25.

8. Schultz, B.E. and S.I. Chan, *Structures and proton-pumping strategies of mitochondrial respiratory enzymes.* Annu Rev Biophys Biomol Struct, 2001. **30**: p. 23-65.

9. Cecchini, G., et al., *Succinate dehydrogenase and fumarate reductase from Escherichia coli.* Biochim Biophys Acta, 2002. **1553**(1-2): p. 140-57.

10. Yu, C.A., et al., *Structure and reaction mechanisms of multifunctional mitochondrial cytochrome bc1 complex.* Biofactors, 1999. **9**(2-4): p. 103-9.

11. Malka, F., A. Lombes, and M. Rojo, *Organization, dynamics and transmission of mitochondrial DNA: focus on vertebrate nucleoids.* Biochim Biophys Acta, 2006. **1763**(5-6): p. 463-72.

12. Ludwig, B., et al., *Cytochrome C oxidase and the regulation of oxidative phosphorylation.* Chembiochem, 2001. **2**(6): p. 392-403.

13. Devenish, R.J., M. Prescott, and A.J. Rodgers, *The structure and function of mitochondrial F1F0-ATP synthases.* Int Rev Cell Mol Biol, 2008. **267**: p. 1-58.

14. Boyer, P.D., *A model for conformational coupling of membrane potential and proton translocation to ATP synthesis and to active transport.* FEBS Lett, 1975. **58**(1): p. 1-6.

15. Contessi, S., et al., *IF(1) distribution in HepG2 cells in relation to ecto-F(0)F (1)ATPsynthase and calmodulin.* J Bioenerg Biomembr, 2007. **39**(4): p. 291-300.

16. Pullman, M.E. and G.C. Monroy, *A Naturally Occurring Inhibitor of Mitochondrial Adenosine Triphosphatase.* J Biol Chem, 1963. **238**: p. 3762-9.

17. Walker, J.E., et al., *Structure and genes of ATP synthase.* Biochem Soc Trans, 1987. **15**(1): p. 104-6.

18. Cabezon, E., et al., *The structure of bovine F1-ATPase in complex with its regulatory protein IF1.* Nat Struct Biol, 2003. **10**(9): p. 744-50.

19. Gledhill, J.R., et al., *Mechanism of inhibition of bovine F1-ATPase by resveratrol and related polyphenols.* Proc Natl Acad Sci U S A, 2007. **104**(34): p. 13632-7.

20. Campanella, M., et al., *IF1, the endogenous regulator of the F(1)F(o)-ATPsynthase, defines mitochondrial volume fraction in HeLa cells by regulating autophagy.* Biochim Biophys Acta, 2009. **1787**(5): p. 393-401.

21. Campanella, M., et al., *Regulation of mitochondrial structure and function by the F1Fo-ATPase inhibitor protein, IF1.* Cell Metab, 2008. **8**(1): p. 13-25.

22. Hall, A.M., et al., *Multiphoton imaging reveals differences in mitochondrial function between nephron segments.* J Am Soc Nephrol, 2009. **20**(6): p. 1293-302.

23. Zanotti, F., et al., *Effect of the ATPase inhibitor protein IF1 on H+ translocation in the mitochondrial ATP synthase complex.* Biochem Biophys Res Commun, 2009. **384**(1): p. 43-8.

24. Kudin, A.P., D. Malinska, and W.S. Kunz, *Sites of generation of reactive oxygen species in homogenates of brain tissue determined with the use of respiratory substrates and inhibitors.* Biochim Biophys Acta, 2008. **1777**(7-8): p. 689-95.

25. Genova, M.L., et al., *The site of production of superoxide radical in mitochondrial Complex I is not a bound ubisemiquinone but presumably iron-sulfur cluster N2.* FEBS Lett, 2001. **505**(3): p. 364-8.

26. Lenaz, G., *The mitochondrial production of reactive oxygen species: mechanisms and implications in human pathology.* IUBMB Life, 2001. **52**(3-5): p. 159-64.

27. Liu, Y., G. Fiskum, and D. Schubert, *Generation of reactive oxygen species by the mitochondrial electron transport chain.* J Neurochem, 2002. **80**(5): p. 780-7.

28. Lambert, A.J. and M.D. Brand, *Superoxide production by NADH:ubiquinone oxidoreductase (complex I) depends on the pH gradient across the mitochondrial inner membrane.* Biochem J, 2004. **382**(Pt 2): p. 511-7.

29. Zelko, I.N., T.J. Mariani, and R.J. Folz, *Superoxide dismutase multigene family: a comparison of the CuZn-SOD (SOD1), Mn-SOD (SOD2), and EC-SOD (SOD3) gene structures, evolution, and expression.* Free Radic Biol Med, 2002. **33**(3): p. 337-49.

30. Chen, L., et al., *Reduction of mitochondrial H2O2 by overexpressing peroxiredoxin 3 improves glucose tolerance in mice.* Aging Cell, 2008. **7**(6): p. 866-78.

31. Park, S.G., et al., *Generation of reactive oxygen species in adipose-derived stem cells: friend or foe?* Expert Opin Ther Targets, 2011. **15**(11): p. 1297-306.

32. Han, C.Y., et al., *NADPH oxidase-derived reactive oxygen species increases expression of monocyte chemotactic factor genes in cultured adipocytes.* J Biol Chem, 2012.

33. Semenza, G.L., *Oxygen-dependent regulation of mitochondrial respiration by hypoxia-inducible factor 1.* Biochem J, 2007. **405**(1): p. 1-9.

34. Wang, G.L., G.S. Zhao, and D.J. Song, *[A study of the effect of fish oils on the risk factors of cardiovascular and cerebrovascular diseases].* Zhonghua Nei Ke Za Zhi, 1992. **31**(4): p. 209-12, 254.

35. Bento, C.F. and P. Pereira, *Regulation of hypoxia-inducible factor 1 and the loss of the cellular response to hypoxia in diabetes.* Diabetologia, 2011. **54**(8): p. 1946-56.

36. Berra, E., et al., *HIF prolyl-hydroxylase 2 is the key oxygen sensor setting low steady-state levels of HIF-1alpha in normoxia.* EMBO J, 2003. **22**(16): p. 4082-90.

37. Hewitson, K.S., C.J. Schofield, and P.J. Ratcliffe, *Hypoxia-inducible factor prolyl-hydroxylase: purification and assays of PHD2.* Methods Enzymol, 2007. **435**: p. 25-42.

38. Lando, D., et al., *FIH-1 is an asparaginyl hydroxylase enzyme that regulates the transcriptional activity of hypoxia-inducible factor.* Genes Dev, 2002. **16**(12): p. 1466-71.

39. Semenza, G.L., *Hypoxia-inducible factor 1: regulator of mitochondrial metabolism and mediator of ischemic preconditioning.* Biochim Biophys Acta, 2011. **1813**(7): p. 1263-8.

40. Hu, C.J., et al., *Differential regulation of the transcriptional activities of hypoxia-inducible factor 1 alpha (HIF-1alpha) and HIF-2alpha in stem cells.* Mol Cell Biol, 2006. **26**(9): p. 3514-26.

41. Kaelin, W.G., Jr. and P.J. Ratcliffe, *Oxygen sensing by metazoans: the central role of the HIF hydroxylase pathway.* Mol Cell, 2008. **30**(4): p. 393-402.

42. Kim, J.W., et al., *HIF-1-mediated expression of pyruvate dehydrogenase kinase: a metabolic switch required for cellular adaptation to hypoxia.* Cell Metab, 2006. **3**(3): p. 177-85.

43. Hamanaka, R.B. and N.S. Chandel, *Mitochondrial reactive oxygen species regulate hypoxic signaling.* Curr Opin Cell Biol, 2009. **21**(6): p. 894-9.

44. Solaini, G., et al., *Hypoxia and mitochondrial oxidative metabolism.* Biochim Biophys Acta, 2010. **1797**(6-7): p. 1171-7.

45. Palacios-Callender, M., et al., *Endogenous NO regulates superoxide production at low oxygen concentrations by modifying the redox state of cytochrome c oxidase.* Proc Natl Acad Sci U S A, 2004. **101**(20): p. 7630-5.

46. Fukuda, R., et al., *HIF-1 regulates cytochrome oxidase subunits to optimize efficiency of respiration in hypoxic cells.* Cell, 2007. **129**(1): p. 111-22.

47. Zhang, H., et al., *Mitochondrial autophagy is an HIF-1-dependent adaptive metabolic response to hypoxia.* J Biol Chem, 2008. **283**(16): p. 10892-903.

48. Tello, D., et al., *Induction of the mitochondrial NDUFA4L2 protein by HIF-1alpha decreases oxygen consumption by inhibiting Complex I activity.* Cell Metab, 2011. **14**(6): p. 768-79.

49. Chan, S.Y., et al., *MicroRNA-210 controls mitochondrial metabolism during hypoxia by repressing the iron-sulfur cluster assembly proteins ISCU1/2.* Cell Metab, 2009. **10**(4): p. 273-84.

50. Chen, Z., et al., *Hypoxia-regulated microRNA-210 modulates mitochondrial function and decreases ISCU and COX10 expression.* Oncogene, 2010. **29**(30): p. 4362-8.

51. Favaro, E., et al., *MicroRNA-210 regulates mitochondrial free radical response to hypoxia and krebs cycle in cancer cells by targeting iron sulfur cluster protein ISCU.* PLoS One, 2010. **5**(4): p. e10345.

52. Jezek, P. and L. Plecita-Hlavata, *Mitochondrial reticulum network dynamics in relation to oxidative stress, redox regulation, and hypoxia.* Int J Biochem Cell Biol, 2009. **41**(10): p. 1790-804.

53. Giacco, F. and M. Brownlee, *Oxidative stress and diabetic complications.* Circ Res, 2010. **107**(9): p. 1058-70.

54. Geraldes, P. and G.L. King, *Activation of protein kinase C isoforms and its impact on diabetic complications.* Circ Res, 2010. **106**(8): p. 1319-31.

55. Vikramadithyan, R.K., et al., *Human aldose reductase expression accelerates diabetic atherosclerosis in transgenic mice.* J Clin Invest, 2005. **115**(9): p. 2434-43.

56. Wautier, J.L. and A.M. Schmidt, *Protein glycation: a firm link to endothelial cell dysfunction.* Circ Res, 2004. **95**(3): p. 233-8.

57. Goldin, A., et al., *Advanced glycation end products: sparking the development of diabetic vascular injury.* Circulation, 2006. **114**(6): p. 597-605.

58. Geraldes, P., et al., *Activation of PKC-delta and SHP-1 by hyperglycemia causes vascular cell apoptosis and diabetic retinopathy.* Nat Med, 2009. **15**(11): p. 1298-306.

59. Williams, B., et al., *Glucose-induced protein kinase C activation regulates vascular permeability factor mRNA expression and peptide production by human vascular smooth muscle cells in vitro.* Diabetes, 1997. **46**(9): p. 1497-503.

60. Pitocco, D., et al., *Oxidative stress, nitric oxide, and diabetes.* Rev Diabet Stud, 2010. **7**(1): p. 15-25.

61. Afanas'ev, M.V., et al., *Molecular typing of Mycobacterium tuberculosis circulated in Moscow, Russian Federation.* Eur J Clin Microbiol Infect Dis, 2011. **30**(2): p. 181-91.

62. Herlein, J.A., et al., *Superoxide and respiratory coupling in mitochondria of insulin-deficient diabetic rats.* Endocrinology, 2009. **150**(1): p. 46-55.

63. Gallagher, K.A., et al., *Diabetic impairments in NO-mediated endothelial progenitor cell mobilization and homing are reversed by hyperoxia and SDF-1 alpha.* J Clin Invest, 2007. 117(5): p. 1249-59.

64. Ceradini, D.J., et al., *Decreasing intracellular superoxide corrects defective ischemia-induced new vessel formation in diabetic mice.* J Biol Chem, 2008. **283**(16): p. 10930-8.

65. Baelde, H.J., et al., *Reduction of VEGF-A and CTGF expression in diabetic nephropathy is associated with podocyte loss.* Kidney Int, 2007. **71**(7): p. 637-45.

66. Catrina, S.B., et al., *Hyperglycemia regulates hypoxia-inducible factor-1alpha protein stability and function.* Diabetes, 2004. **53**(12): p. 3226-32.

67. Xue, W., et al., *Cardiac-specific overexpression of HIF-1{alpha} prevents deterioration of glycolytic pathway and cardiac remodeling in streptozotocin-induced diabetic mice.* Am J Pathol, 2010. **177**(1): p. 97-105.

68. Botusan, I.R., et al., *Stabilization of HIF-1alpha is critical to improve wound healing in diabetic mice.* Proc Natl Acad Sci U S A, 2008. **105**(49): p. 19426-31.

69. Sarkar, K., et al., *Adenoviral transfer of HIF-1alpha enhances vascular responses to critical limb ischemia in diabetic mice.* Proc Natl Acad Sci U S A, 2009. **106**(44): p. 18769-74.

70. Nagy, G., et al., *Association of hypoxia inducible factor-1 alpha gene polymorphism with both type 1 and type 2 diabetes in a Caucasian (Hungarian) sample.* BMC Med Genet, 2009. **10**: p. 79.

71. Thangarajah, H., et al., *The molecular basis for impaired hypoxia-induced VEGF expression in diabetic tissues.* Proc Natl Acad Sci U S A, 2009. **106**(32): p. 13505-10.

72. Bento, C.F., et al., *The chaperone-dependent ubiquitin ligase CHIP targets HIF-1alpha for degradation in the presence of methylglyoxal.* PLoS One, 2010. **5**(11): p. e15062.

73. Luo, W., et al., *Hsp70 and CHIP selectively mediate ubiquitination and degradation of hypoxia-inducible factor (HIF)-1alpha but Not HIF-2alpha.* J Biol Chem, 2010. **285**(6): p. 3651-63.

74. Chen, Y.C., et al., *The effects of altitude training on the AMPK-related glucose transport pathway in the red skeletal muscle of both lean and obese Zucker rats.* High Alt Med Biol, 2011. **12**(4): p. 371-8.

75. Schofield, C.J. and P.J. Ratcliffe, *Oxygen sensing by HIF hydroxylases.* Nat Rev Mol Cell Biol, 2004. **5**(5): p. 343-54.

76. Semenza, G.L., *Regulation of vascularization by hypoxia-inducible factor 1.* Ann N Y Acad Sci, 2009. **1177**: p. 2-8.

77. Denko, N.C., *Hypoxia, HIF1 and glucose metabolism in the solid tumour.* Nat Rev Cancer, 2008. **8**(9): p. 705-13.

78. Weinberg, F. and N.S. Chandel, *Reactive oxygen species-dependent signaling regulates cancer.* Cell Mol Life Sci, 2009. **66**(23): p. 3663-73.

79. Fandrey, J., S. Frede, and W. Jelkmann, *Role of hydrogen peroxide in hypoxia-induced erythropoietin production.* Biochem J, 1994. **303 (Pt 2)**: p. 507-10.

80. Agani, F.H., et al., *The role of mitochondria in the regulation of hypoxia-inducible factor 1 expression during hypoxia.* J Biol Chem, 2000. **275**(46): p. 35863-7.

81. Chandel, N.S., et al., *Mitochondrial reactive oxygen species trigger hypoxia-induced transcription.* Proc Natl Acad Sci U S A, 1998. **95**(20): p. 11715-20.

82. Chavez, A., et al., *Mitochondria and hypoxia-induced gene expression mediated by hypoxia-inducible factors.* Ann N Y Acad Sci, 2008. **1147**: p. 312-20.

83. Thomas, R.L., D.A. Kubli, and A.B. Gustafsson, *Bnip3-mediated defects in oxidative phosphorylation promote mitophagy.* Autophagy, 2011. **7**(7): p. 775-7.

84. Brownlee, M., *Biochemistry and molecular cell biology of diabetic complications.* Nature, 2001. **414**(6865): p. 813-20.

85. Nishikawa, T., D. Edelstein, and M. Brownlee, *The missing link: a single unifying mechanism for diabetic complications.* Kidney Int Suppl, 2000. **77**: p. S26-30.

86. Li, W., et al., *Extracellular heat shock protein-90alpha: linking hypoxia to skin cell motility and wound healing.* EMBO J, 2007. **26**(5): p. 1221-33.

87. Gao, W., et al., *High glucose concentrations alter hypoxia-induced control of vascular smooth muscle cell growth via a HIF-1alpha-dependent pathway.* J Mol Cell Cardiol, 2007. **42**(3): p. 609-19.

88. Ha, H., et al., *Role of reactive oxygen species in the pathogenesis of diabetic nephropathy.* Diabetes Res Clin Pract, 2008. **82 Suppl 1**: p. S42-5.

89. Zheng, L. and T.S. Kern, *Role of nitric oxide, superoxide, peroxynitrite and PARP in diabetic retinopathy.* Front Biosci, 2009. **14**: p. 3974-87.

90. Munusamy, S. and L.A. MacMillan-Crow, *Mitochondrial superoxide plays a crucial role in the development of mitochondrial dysfunction during high glucose exposure in rat renal proximal tubular cells.* Free Radic Biol Med, 2009. **46**(8): p. 1149-57.

91. Bindokas, V.P., et al., *Visualizing superoxide production in normal and diabetic rat islets of Langerhans.* J Biol Chem, 2003. **278**(11): p. 9796-801.

92. Chaanine, A.H., et al., *JNK modulates FOXO3a for the expression of the mitochondrial death and mitophagy marker BNIP3 in pathological hypertrophy and in heart failure.* Cell Death Dis, 2012. **3**: p. 265.

93. Scherz-Shouval, R. and Z. Elazar, *ROS, mitochondria and the regulation of autophagy.* Trends Cell Biol, 2007. **17**(9): p. 422-7.

94. Sanchez-Cenizo, L., et al., *Up-regulation of the ATPase inhibitory factor 1 (IF1) of the mitochondrial H+-ATP synthase in human tumors mediates the metabolic shift of cancer cells to a Warburg phenotype.* J Biol Chem, 2010. **285**(33): p. 25308-13.

95. Grover, G.J., et al., *Excessive ATP hydrolysis in ischemic myocardium by mitochondrial F1F0-ATPase: effect of selective pharmacological inhibition of mitochondrial ATPase hydrolase activity.* Am J Physiol Heart Circ Physiol, 2004. **287**(4): p. H1747-55.

96. Trounce, I.A., et al., *Assessment of mitochondrial oxidative phosphorylation in patient muscle biopsies, lymphoblasts, and transmitochondrial cell lines.* Methods Enzymol, 1996. **264**: p. 484-509.

97. Baracca, A., et al., *Biochemical phenotypes associated with the mitochondrial ATP6 gene mutations at nt8993.* Biochim Biophys Acta, 2007. **1767**(7): p. 913-9.